



# Isotope record of groundwater recharge mechanisms and climate change in southwestern North America



C.J. Eastoe

Department of Geosciences, University of Arizona, Tucson, AZ, 85721, USA

## ARTICLE INFO

Editorial handling by: Benjamin Silas gilfedder

**Keywords:**

Groundwater age  
Stable water isotopes  
Carbon-14  
Recharge mechanisms  
Climate change  
Southwestern north America

## ABSTRACT

Understanding the response of groundwater systems to changes in climate is crucial at a time when human-caused climate change appears to be increasing in magnitude and rate. Groundwater preserves records of past effects resulting from climate change at the time-scale of late Pleistocene-Holocene climate evolution. Detailed regional datasets provide opportunities for evaluating past changes as a means of anticipating future climate-groundwater relations. Isotope parameters  $\delta^{18}\text{O}$ ,  $\delta^2\text{H}$  and uncorrected  $^{14}\text{C}$ , considered together in large groundwater datasets from southwestern North America, provide evidence of changes in groundwater recharge mechanisms and the climate changes that led to them. The evidence consists in positive shifts in  $\delta^{18}\text{O}$  and  $\delta^2\text{H}$  in paleowater recharge related to a 13–15 ka shift recorded in  $\delta^{18}\text{O}$  of speleothem deposits, and as concurrent changes in recharge seasonality in the core area of the North American monsoon. A negative shift in  $\delta^{18}\text{O}$  and  $\delta^2\text{H}$ , most likely contemporaneous with a regional 51–55 ka change speleothem deposits, is recorded in certain basins with deep, confined groundwater. A  $^{14}\text{C}$  threshold of 10 percent modern carbon serves empirically to distinguish paleowaters before and after the 13–15 ka event. A younger, negative isotope shift has occurred in Baja California. The 13–15 ka shift is regional but is not recorded in all basins studied and appears to be absent at the northwestern and southeastern limits of the study area. Relations among the isotope parameters may be complicated by factors such as isotope altitude effects, delayed melting of Pleistocene ice, changing degrees of evaporation in river water and introduction of anthropogenic  $^{14}\text{C}$ . Recharge mechanisms fall into two patterns: (1) dominant winter recharge with varying degrees of evaporation prior to infiltration, and (2) recharge in both summer and winter, but only during the wettest months. Pattern (2) replaced pattern (1) at 13–15 ka in the core area of the North American monsoon. Later, the present-day pattern of recharge from summer-fall rain associated with tropical depressions replaced predominant winter recharge in southern and eastern Baja California. A post-1950 negative shift in  $\delta^{18}\text{O}$  and  $\delta^2\text{H}$ , observed in southern Nevada and northern New Mexico, may be of anthropogenic origin and related to development of large-scale irrigation in California.

## 1. Introduction

Ancient, or fossil, groundwater, originating as pre-Holocene recharge, is common across the globe (Clark and Fritz, 1997; Jasechko et al., 2017; and references in those articles). Such groundwater preserves a record of past climate regimes in which recharge fluxes and mechanisms may have differed greatly from those obtaining at present. Fossil groundwater is a crucial source of domestic and agricultural water supply. In the context of anticipated climate change arising from human activities, it is important to understand how recharge responds to major shifts in climate. Where isotope datasets exist for multiple groundwater basins in a given region, possibilities for understanding the effects of climate change on groundwater emerge from detailed comparison of the

data.

Within 1000 m of the surface, fossil groundwater makes up 42–85% of the total storage in groundwater basins reviewed by Jasechko et al. (2017), and within 300 m of the surface, 22–74%. These ranges are based on corrected groundwater  $^{14}\text{C}$  activity, with a threshold of 11,700 years. The stable O and H isotope composition of such groundwater commonly differs from that of younger recharge as a result of climate change near the Pleistocene-Holocene transition. Positive shifts of  $\delta^{18}\text{O}$ , i.e.  $\delta^{18}\text{O}$  (late Pleistocene) <  $\delta^{18}\text{O}$  (Holocene), are most common, occurring in 82% of the case-studies reviewed by Jasechko (2019), but negative shifts are recorded in certain tropical, coastal aquifers. In the western USA, isotope shifts documented in Fig. 25 of Jasechko (2019) are positive.

E-mail address: [eastoe@email.arizona.edu](mailto:eastoe@email.arizona.edu).

Using stable O and H isotopes in conjunction with  $^{14}\text{C}$ , Phillips et al. (1986) noted that groundwater from the San Juan Basin on the Colorado Plateau had undergone a shift in stable isotope composition at a time near the Pleistocene-Holocene transition. The authors attributed the shift, about 2‰ in  $\delta^{18}\text{O}$ , to change in the isotope composition of precipitation in response to climatic warming at the end of the most recent global glaciation. In southwestern North America, U-series dating of speleothems places shifts of 2–3‰ in  $\delta^{18}\text{O}$  of cave drip-water at 13–15 Ka at the Cave of the Bells, southern Arizona (Wagner et al., 2010), and near 15 ka at Fort Stanton Cave, southeastern New Mexico (Asmerom et al., 2010). A similar isotope shift is found at 10–12 ka in Greenland ice, where the date is based on ice-layer chronology (Johnsen et al., 2001).

Isotope shifts in precipitation elsewhere have been documented using  $\delta^{18}\text{O}$  and  $\delta^2\text{H}$  of groundwater,  $^{14}\text{C}$  of dissolved inorganic carbon (DIC) and  $\delta^{18}\text{O}$  in dated speleothem material, but may have occurred at different times (Clark and Fritz, 1997; Jasechko et al., 2015; Jiang et al., 2019). Establishment of precise and reliable residence times for groundwater from  $^{14}\text{C}$  measurements on DIC is problematic, given uncertainties as to the isotope composition of DIC sources and complexity in their evolution following recharge, in combination with uncertainties as to the isotope composition of potential sampling problems (Clark and Fritz, 1997; Cartwright et al., 2020). Nonetheless, detailed datasets of  $\delta^{18}\text{O}$ ,  $\delta^2\text{H}$  and uncorrected  $^{14}\text{C}$  in groundwater potentially contain information about recharge mechanisms in addition to climate change. Numerous such datasets are available for southwestern North America. In this study, the datasets are systematically examined for detailed relationships among the three parameters. The aims are: (1) to determine whether a late Pleistocene/early Holocene shift in  $\delta^{18}\text{O}$  and  $\delta^2\text{H}$  precipitation was regional in extent; (2) to investigate changes in groundwater recharge mechanism concurrent with the isotope shift; (3) to interpret the findings in terms of changing climate pattern and, where possible, moisture source; and (4) to relate the groundwater and speleothem records.

## 2. Background

### 2.1. Study area

The datasets reviewed here span the area shown in Fig. 1, mostly in the North American Cordillera. The area is semiarid to arid, except at high elevations. Long-term data for recent climate (Table 1) show that along the Pacific coast, in southern Nevada and in northern Arizona, most precipitation falls from late autumn to spring, when Pacific frontal weather systems dominate moisture transport. Elsewhere, summer or early autumn precipitation predominates. In Baja California Sur, Sonora, Chihuahua, Arizona and New Mexico, convective precipitation associated with the North American monsoon provides rainfall between June and September, the amount waning northward. In the same area, tropical cyclonic weather systems from the Pacific Ocean also provide summer and early autumn precipitation that is reliable each year only in areas near the southern end of the Gulf of California. Precipitation in June–October accounts for almost 80% of annual precipitation in southern parts of the study area and 44–70% elsewhere except for stations in southern Nevada and southern California (Table 1).

Much of the study area lies within the Basin and Range Province (Fenneman, 1931) where basin-fill alluvium makes up large regional aquifers. Other kinds of aquifers are also represented in the study: Neogene to Quaternary sediments of coastal and intermontane basins along the West Coast, the Neogene Ogallala Formation of the High Plains and approximately flat-lying Paleozoic and Mesozoic strata of the Colorado Plateau and High Plains. A few data are from fractured hard-rock and karst aquifers.

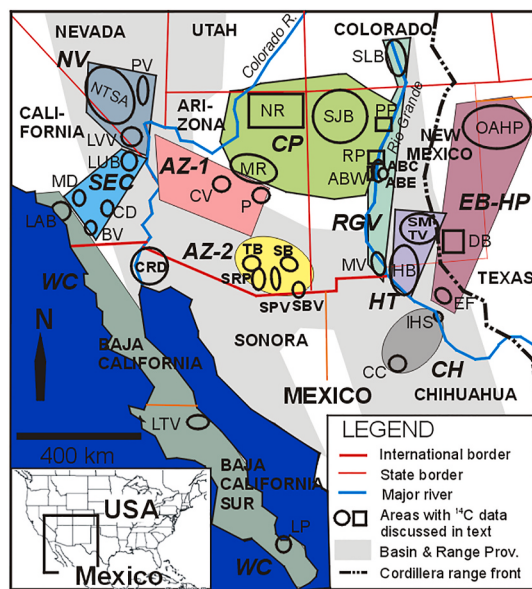


**Fig. 1.** Map of southwestern North America, showing locations mentioned in this study, classified into broad regions (colored shapes). Abbreviations are as follows. Region AZ-1 (Arizona, Pattern 1): CV = Chino Valley, P = Payson. Region AZ-2 (Arizona, Pattern 2): SB = Safford Basin, SBV = San Bernardino Valley, SPV = San Pedro Valley, SRF = Santa Rita to Patagonia Mountains, TB = Tucson Basin. Region CH (Chihuahua): CC = Ciudad Chihuahua, IHS = Indian Hot Springs. Region CP (Colorado Plateau): MR = Mogollon Rim, NR = Navajo Reservation, PP = Pajarito Plateau, SJB = San Juan Basin. Region EB-HP (Eastern Basins-High Plains): DB = Delaware Basin, EF = Eagle Flat, OAH = Ogallala Aquifer High Plains. Region HT (Hueco Bolson-Tularosa Valley): HB = Hueco Bolson, SMTV = Sacramento Mountains-Tularosa Valley. Region NV (southern Great Basin, Nevada): LLV = Las Vegas Valley, NTSA = Nuclear Test Site-Amargosa, PV = Pahrangat Valley. Region SEC (southeastern California: BV = Borrego Valley, CD = Central Deserts, LUB = Low-use basins, MD = Mojave Desert; Region RGV (Rio Grande Valley) ABC, ABE, ABW = Albuquerque Basin Central, East and West, MV = Mesilla Valley, RP = Rio Puerco, SLB = San Luis Basin. Region WC (West Coast): LAB = Los Angeles Basin, LP = La Paz, LTV = Las Tres Vírgenes. CRD = Colorado River delta.

### 2.2. Previous work

Publications from which data are drawn are reviewed below. In addition to these sources, the following studies at regional scale are relevant to the present work.

Recharge mechanisms in alluvial aquifers of Arizona show regional zonation (Eastoe and Towne, 2018). Where local recharge predominates (i.e., where recharge of isotopically-distinctive water conveyed by major streams from beyond the basin boundary is insignificant), one of two patterns of O and H isotope data occurs. Pattern 1, in northwestern Arizona, consists in recharge of winter precipitation only, with different degrees of evaporation and no evidence of an isotope altitude effect in the winter precipitation. This regime prevails despite approximately equal proportions of summer and winter precipitation and the occurrence of runoff in summer. Pattern 2, in southeastern and southern Arizona, consists in recharge of a mixture of summer and winter precipitation from the wettest 30% (approximately) of months. Eastoe and Towne (2018) identified three basins in west-central Arizona where the zone of Pattern 2 recharge has moved northward, overprinting Pattern 1 recharge. Patterns 1 and 2 are also present in fractured-rock aquifers of the mountain blocks of Arizona (Eastoe and Wright, 2019). Pattern 1 is thought to extend along the southern rim of the Colorado Plateau, where it is expressed in groundwater supplying base flow of major rivers (Eastoe and Towne, 2018). These articles suggested the possibility of regional patterns of recharge mechanisms extending beyond Arizona, and that such mechanisms might have changed at time scales from

**Table 1**

Precipitation by month at representative stations in the study area.

Site	State	Region (Fig. 1)	Lat. °	Long. °	Elev. masl	J mm	F mm	M mm	A mm	M mm	J mm	J mm	A mm	S mm	O mm	N mm	D mm	Annual mm	% J-O
Los Angeles APT	CA	WC	33.94	-118.41	58	67	68	47	20	4	1	1	2	4	10	36	46	305	6
Mt Baldy Notch	CA	WC	34.27	-117.61	2370	215	198	94	117	21	2	9	9	31	17	145	167	1025	7
La Paz	BCS	WC	28.634	-106.07	31	8	7	1	0	0	2	13	28	65	14	13	12	163	75
Las Vegas APT NV	NV	NV	36.08	-115.16	649	13	14	11	5	4	2	11	11	8	7	9	10	105	37
Red Rock State Park	NV	NV	36.14	-115.43	1146	45	56	48	15	6	3	25	28	14	13	19	23	296	28
Prescott APT	AZ	AZ-1	34.65	-112.43	1531	24	18	20	14	7	11	71	67	27	21	17	28	325	61
Tucson APT	AZ	AZ-2	32.12	-110.94	791	22	20	18	8	6	7	60	56	33	21	17	24	291	61
Mt Lemmon	AZ	AZ-2	32.44	-110.79	2791	58	33	90	38	10	32	185	173	36	24	46	37	762	59
Flagstaff	AZ	CP	35.14	-111.68	2134	53	51	52	32	16	11	63	69	49	38	41	52	525	44
Farmington APT	NM	CP	36.74	-108.23	1610	14	12	13	14	12	8	21	28	20	29	12	20	204	52
Alamosa APT	CO	RGV	37.44	-105.86	2300	7	7	11	13	16	13	27	30	21	17	9	9	179	60
Albuquerque APT	NM	RGV	35.05	-106.62	1621	9	10	13	14	15	15	36	37	24	22	11	12	220	61
Sandia Park	NM	RGV	35.17	106.37	2172	32	29	40	25	27	26	74	78	45	40	34	31	481	55
El Paso APT	TX	HT	31.80	-106.40	1199	10	11	7	5	9	18	41	39	36	17	10	15	217	69
Cloudcroft	NM	HT	32.96	-105.74	2643	43	39	39	20	27	47	130	128	70	44	30	43	659	63
Alamogordo	NM	HT	32.90	-105.94	1347	16	14	12	9	13	20	45	52	39	26	14	18	278	65
Cd. Chihuahua	CHIH	CH	28.63	-106.07	1442	11	8	7	8	13	22	75	74	64	25	16	9	332	78
Van Horn	TX	EB-HP	31.041	-104.83	1235	13	9	5	8	15	24	50	51	47	27	13	13	275	72
Lubbock APT	TX	EB-HP	33.65	-101.83	1002	13	14	21	46	67	71	58	43	59	54	15	18	479	60

JFMAMJJASOND = months of the year.

Data from: USA –Western Regional Climate Center (2021), Mexico – Climate-data.org (2021)

State abbreviations: AZ = Arizona, BCS = Baja California Sur, CA = California, CHIH = Chihuahua, CO = Colorado, NM = New Mexico, NV = Nevada, TX = Texas.

%J-O is the percentage of annual precipitation falling from June to October.

APT = airport.

Elev. masl = elevation, m above sea level.

decadal to millennial.

Long-distance (up to 200 km) groundwater flow allows mixing of waters of wide-ranging residence time along flow paths and may confuse relationships between  $^{14}\text{C}$  and stable isotope parameters. Such long-distance flow occurs through and between elongate alluvial basins of the Basin and Range Province in southwestern Nevada, where continuous, permeable carbonate and tuff strata occur in hard-rock mountain ranges (Winograd and Friedman, 1972; Winograd and Thordarson, 1975; Winograd and Pearson, 1976; Davission et al., 1999). Flowpaths of similar scale, 100–200 km, occur in carbonate strata east of the crest of the Sacramento Mountains, New Mexico (Newton et al., 2012; Eastoe and Rodney, 2014) and between alluvial basins in the Basin and Range Province in Trans-Pecos Texas (Uliana and Sharp, 2001). Inter-basin flow paths of similar extent are not thought to occur in other areas of the Basin and Range Province, where impermeable silicate rocks predominate in the ranges and complex structures dismember permeable strata.

### 2.3. Preservation of isotope input signals by groundwater systems

Groundwater and its solutes evolve in complex fashion. A particular volume of groundwater is likely to consist of a mixture of aliquots of different residence time because of flow along a multitude of paths at a variety of spatial and temporal scales. In systems of adjacent aquifers and aquiclude, water isotopes and solutes may disperse from moving water into stationary water (Davidson and Airey, 1982). A further form of mixing arises where samples are taken from wells with long screens

drawing water of a variety of residence times and compositions. Groundwater and sampling techniques therefore constitute a low-pass filter, attenuating output signals (those detected in sample sets) relative to input signals such as changes in O and H isotope composition of precipitation (Cartwright, 1982). Groundwater of long residence time (thousands to tens-of-thousands of years) is therefore likely to preserve attenuated output signals corresponding to large-amplitude or long-period changes such as the Late Pleistocene isotope shift in precipitation, but not signals related to low-amplitude or short-period phenomena. Groundwater of short residence time may, however, preserve evidence of short-period input signals of sufficient amplitude.

A related set of problems applies to the use of  $^{14}\text{C}$  activity measurements to determine groundwater residence times. Measured  $^{14}\text{C}$  activity represents a volume-weighted mean of contributions from the components of each mixture, and calculated residence times, after correction for addition of rock carbon, approximate mean residence times (Cartwright et al., 2020). Correction protocols do not in general take account of mixing of water of different residence times. Dispersion of  $^{14}\text{C}$  into stationary groundwater, analogous to solute effects described by Davidson and Airey (1982), leads to underestimation of residence times (Cartwright et al., 2020). Further uncertainty arises from inadequate knowledge of the parameters required for correction of measured  $^{14}\text{C}$  activities to activities of  $^{14}\text{C}$  in recharge (Clark and Fritz, 1997; Cartwright et al., 2020). For these reasons, it is usually difficult to relate values of  $^{14}\text{C}$  activity to residence times expressed in calendar years.

**Table 2**

Previously unpublished data.

A. GROUNDWATER, INDIAN HOT SPRINGS TEXAS/CHIHUAHUA									
Name	Date	Latitude	Longitude	$\delta^{18}\text{O}$ ‰	$\delta^{2\text{H}}$ ‰	$\delta^{13}\text{C}$ ‰	$^{14}\text{C}$ pMC	Error pMC ( $1\sigma$ )	3H TU
Spring near Soda Spring	1/4/2003	30.828	-105.317	-7.9	-57		8.9	0.14	
Squaw Spring	18/05/2003	30.824	-105.315	-6.6	-55	-1.3	1.3	0.13	<0.8
Chief Spring	18/05/2003	30.824	-105.316	-7.0	-57	-1.7	1.7	0.13	<0.4
IHS Well	18/05/2003	30.824	-105.316	-8.8	-62	-6.6	2.6	0.14	<0.5
Red Bull Spring	18/05/2003	30.861	-105.341	-8.8	-62	-6.6	4.9	0.12	<0.5
Ojos Calientes dug well	18/05/2003	30.825	-105.320	-6.7	-49	-11.4	100.3	0.44	4.1 ± 0.3
Analytical precision ( $1\sigma$ )				0.08	0.9	0.15			
B. SEASONAL PRECIPITATION AGGREGATES, PAYSON, ARIZONA									
Season	Year			$\delta^{18}\text{O}$ ‰	$\delta^{2\text{H}}$ ‰	$\delta^{18}\text{O}$ ‰	$\delta^{2\text{H}}$ ‰		
Winter	2002–2003			-12.9	-90			-6.4	-43
Summer	2003								
Winter	2003–2004			-9.7	-65			-6.6	-45
Summer	2004								
Winter	2004–2005			-12.2	-81			-5.4	-39
Summer	2005								
Winter	2005–2006			-14.0	-93			-6.3	-43
Summer	2006								
Winter	2006–2007			-11.2	-75			-7.3	-51
Summer	2007								
Winter	2007–2008			-12.7	-87			-10.3	-75
Summer	2008								
Winter	2008–2009			-10.5	-66			-7.5	-48
Summer	2009								
Winter	2009–2010			-10.3	-65			-12.0	-84
Summer	2010								
Winter	2010–2011			-12.6	-85			-7.1	-47
Summer	2011								
Winter	2011–2012			-11.0	-67				
Analytical precision ( $1\sigma$ )				0.08	0.9	0.08		0.9	
Means, arithmetic				-11.7	-77.4	-7.7		-52.8	

Winter: November–May.

Summer: June–October.

### 3. Methods

#### 3.1. Sources of data

All data are previously published, except those in Table 2. Details of analytical method and precision may be found in each reference; stable isotope data are reported relative to VSMOW in most papers, or SMOW in older articles. In general, analytical precisions ( $1\sigma$ ) of  $\delta^{18}\text{O}$  and  $\delta^2\text{H}$  are respectively 0.1‰ and 1‰ or better, except for some data published before about 1995. Detection limits ( $0 + 2\sigma$ ) for  $^{14}\text{C}$  measurements are 4 percent modern carbon (pMC) or better for liquid scintillation measurements, and 0.2 pMC for accelerator mass spectrometer measurements. Locations of aquifers mentioned here are shown in Fig. 1.

#### 3.2. Use of data

The chosen datasets report  $\delta^{18}\text{O}$ ,  $\delta^2\text{H}$  and  $^{14}\text{C}$  activity expressed as pMC for numerous samples and have wide ranges of  $^{14}\text{C}$  activity, ideally including some values  $< 10$  pMC. A few additional datasets that did not meet these requirements also proved useful.

In each dataset, values of  $\delta^{18}\text{O}$  and  $\delta^2\text{H}$  are sorted with respect to  $^{14}\text{C}$  activity expressed as pMC. Uncorrected  $^{14}\text{C}$  activity is used because a consistent approach to correction using  $\delta^{13}\text{C}$  values is not possible across the study area. Correction of measured  $^{14}\text{C}$  activities requires information about average values of  $\delta^{13}\text{C}$  in soil carbonate. These cannot be assumed; where available, they range over at least 9‰ across the study area (Eastoe et al., 2016; author's unpublished data). Therefore the approach to using  $^{14}\text{C}$  activity is empirical: a threshold value that separates  $\delta^{18}\text{O}$  and  $\delta^2\text{H}$  data according to magnitude and recharge mechanism has been derived for southern Arizona, and then applied elsewhere. The threshold value of  $^{14}\text{C}$  activity cannot be converted accurately to a residence time to compare with the speleothem data, for reasons described in section 2.3.

Customary  $\delta^2\text{H}$  vs.  $\delta^{18}\text{O}$  plots are used, with data points coded for  $^{14}\text{C}$  activity expressed as pMC. Data are presented below grouped according to the regions shown in Fig. 1. Data are compared with the global meteoric water line (GMWL) of Craig (1961).

Potential problems anticipated at the outset of the study include: (1) post-infiltration changes in  $^{14}\text{C}$  activity as described in Section 2.3, and (2) ambiguity between temporal and altitude-related differences in  $\delta^{18}\text{O}$  and  $\delta^2\text{H}$  in basins with large elevation ranges. Southern Arizona is used as a test case in evaluating both problems. Evidence for these and other possible problems is discussed below.

### 4. Results

The results for this paper consist in new plots of previously-published data, plus data listed in Table 2. For each area, a brief summary of local hydrogeology accompanies the results.

#### 4.1. Area AZ-2, Southern Arizona

Datasets are available for Tucson Basin (Kalin, 1994; Eastoe et al., 2004; Eastoe and Gu, 2016; Eastoe and Wright, 2019), the northern Santa Rita Mountains (Mts.), Cienega Creek Basin and the Patagonia Mts. (Montgomery and Associates, 2009; Tucci, 2018; Schrag-Toso, 2020), San Pedro Basin (Baillie et al., 2007; Hopkins et al., 2014), Safford Basin (Smalley, 1983; Harris, 1999; Eastoe and Towne, 2018) and San Bernardino Basin (Earman, 2004). All data are for groundwater from alluvial basins in the Basin and Range Province, except for a few data from fractured hard-rock aquifers in the Tucson, Santa Rita and Patagonia Mts. In this area, Pattern 2 recharge occurs at present (Eastoe and Towne, 2018).

In Tucson Basin (Fig. 2a), samples with  $< 10$  pMC have lower values of  $\delta^{18}\text{O}$  and  $\delta^2\text{H}$  than those with pMC  $> 10$ , and the former appear to form an evaporation trend. A few samples with 10–40 pMC overlap the

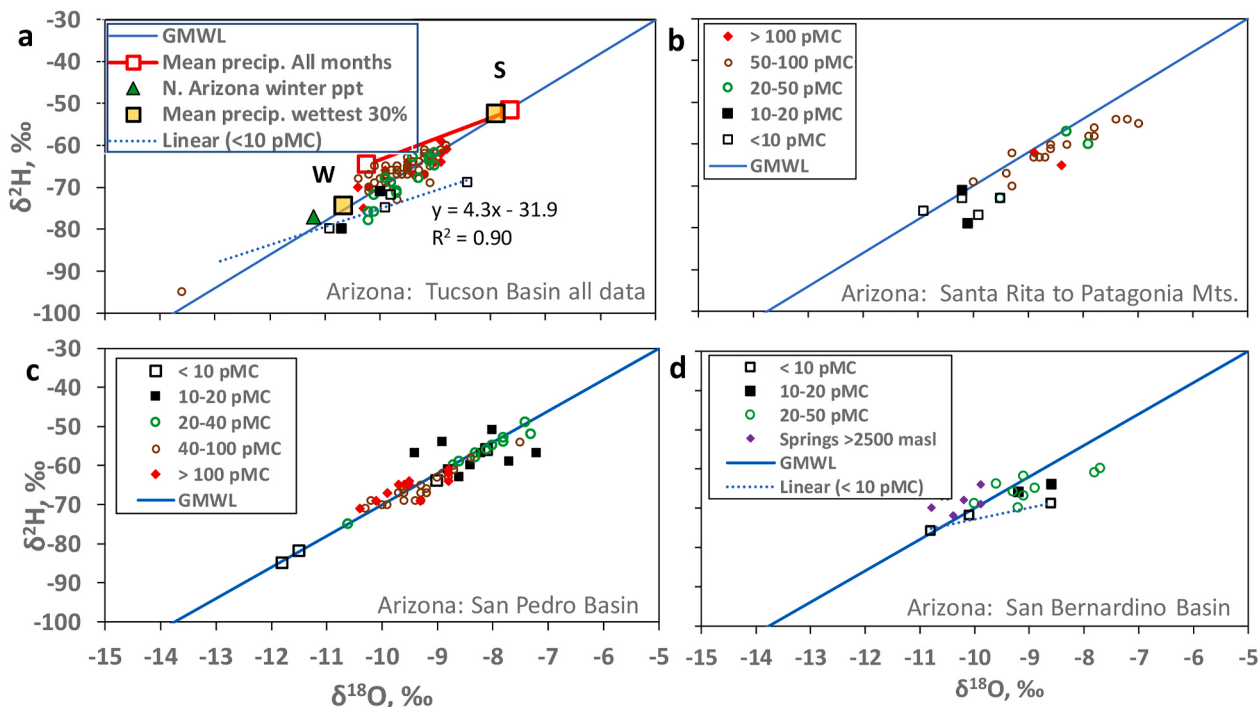


**Fig. 2.**  $\delta^2\text{H}$  vs.  $\delta^{18}\text{O}$ , with data classified for  $^{14}\text{C}$  activity expressed as pMC in region AZ-2. a. Tucson Basin (data of Kalin, 1994; Eastoe et al., 2004; Eastoe and Gu, 2016, Eastoe and Wright, 2019). b. Santa Rita and Patagonia Mountains, south of Tucson (Montgomery and Associates, 2009; Tucci, 2018; Schrag-Toso, 2020). c. San Pedro Basin (Baillie et al., 2007; Hopkins et al., 2014). d. Safford Basin (Smalley, 1983; Harris, 1999; Eastoe and Towne, 2018). Mean isotope compositions of precipitation (precip.) are interpolated from Tucson Basin data for 1800 masl, the altitude at which volumes of precipitation above and below on the Santa Catalina Mountains are about equal (Eastoe and Wright, 2019). Means for all months represent all data, and means for “wettest 30%” represent data for the wettest 30% of months (see Eastoe and Towne, 2018, for a full explanation).

samples with  $<10$  pMC. Eastoe and Wright (2019) considered bulk runoff into Tucson Basin from all altitudes of neighboring high mountains to have a present-day isotope composition corresponding to precipitation at 1800 m above sea level (masl). The source water of the evaporation trend is not present-day winter precipitation at 1800 masl, either for all precipitation or for the wettest 30% of months. Similar patterns are present in the Santa Rita and Patagonia Mts. (Fig. 2b), San Pedro Basin (Fig. 2c), and San Bernardino Basin (Fig. 2d). In the San Pedro Basin, the two groundwater samples that have pMC  $<10$  (specifically, 4.8 and 1.2 pMC) and  $\delta^{18}\text{O}$  and  $\delta^2\text{H}$  data overlapping those of younger groundwater (Fig. 2c) were obtained from aquifers confined beneath up to 200 m of clay and possibly retaining very ancient groundwater (Hopkins et al., 2014). No systematic relations are observed among data with pMC  $>10$ , except in San Pedro Basin, where samples with 10–40 pMC have higher values of  $\delta^{18}\text{O}$  and  $\delta^2\text{H}$  than samples with pMC  $>40$ .

Safford Basin has relatively few  $^{14}\text{C}$  data (Smalley, 1983; Eastoe and Towne, 2018). The samples with pMC  $<10$  are warm, saline waters confined beneath a clay aquitard (Harris, 1999). In Supplementary Fig. S1, samples with  $<10$  pMC are compared with other hot and saline samples of similar origin and thus likely to be old, but lacking  $^{14}\text{C}$  data. In general, they overlap with samples having  $<10$  pMC.

The Tucson Basin data fall into two groups, a larger set (with pMC  $>10$ ) showing the pattern 2 recharge mechanism, and a smaller set (with pMC  $<10$ ) apparently forming an evaporation trend. The separation of samples with  $<10$  and  $>10$  pMC is clearer elsewhere in southern Arizona, as in the northern Santa Rita and Patagonia Mountains (Fig. 2b) where maximum elevations are 1700 masl, but less so in the Tucson and San Bernardino Basins (Fig. 2a, d), where maximum altitudes exceed 2700 masl. In the AZ-2 area as a whole, data with  $<10$  pMC form a broad evaporation trend intersecting the GMWL at  $\delta^{18}\text{O}$  values between  $-11$  and  $-12\text{\textperthousand}$  (Fig. 3). The trend resembles Pattern 1 recharge. The slope is about 4, and the source water cannot be explained as present-day high-altitude recharge represented by spring water discharging above 2500 masl (Fig. 3; data from Cunningham et al., 1998; Earman, 2004).

A threshold value of 10 pMC, uncorrected, is an acceptable criterion in area AZ-2 for distinguishing ancient water recharged under conditions different from those operating at present. If the evaporation trend represents winter recharge, as for present-day pattern 1 recharge in Arizona, the input values of  $\delta^{18}\text{O}$  increased by 1–2% at the threshold, identifiable with the 13–15 ka shift isotope shift in a speleothem in area AZ-2 (Wagner et al., 2010). The 10 pMC threshold will be applied in other parts of the study area.

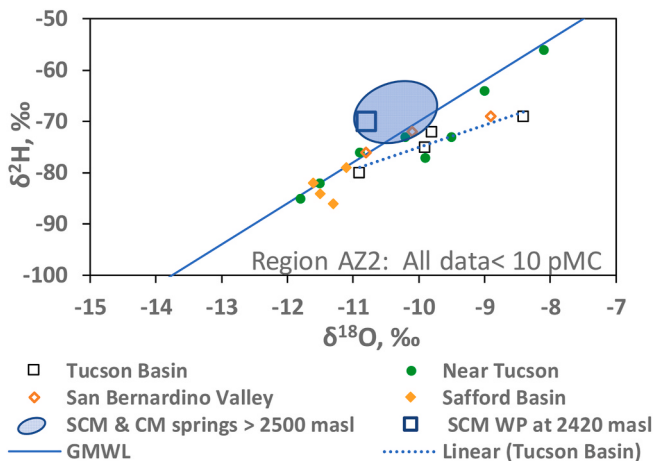


Fig. 3.  $\delta^2\text{H}$  vs.  $\delta^{18}\text{O}$  for all samples with pMC  $<10$  in Region AZ-2. The “Near Tucson” group includes data from Fig. 2b and c. Data sources as for Fig. 2, plus Earman (2004). CM = Chiricahua Mts., SCM = Santa Catalina Mts., SRM = Santa Rita Mts., WP = Winter precipitation.

#### 4.2. Area AZ-1, central-Northwestern Arizona

The datasets represent alluvial aquifers of the Basin and Range Province and the Transition Zone between that province and the Colorado Plateau (Eastoe and Towne, 2018) and fractured hard-rock aquifers at Payson (Eastoe, 2007) and Chino Valley (Wirt and DeWitt, 2005). For Chino Valley, only data from the southwest flank, where local recharge is certain (as opposed to the northeast flank, where recharge may have occurred at remote sites on the Colorado Plateau), are used. Eastoe and Towne (2018) recognized present-day Pattern 1 recharge plotting as a set of similar evaporation trends, combined in Fig. 4, that originate near the point ( $-11.2$ ,  $-77\text{\textperthousand}$ ). The authors suggested that a subset of the data, encountered in most of the basins studied and plotting on a separate evaporation trend below the Pattern 1 trend, represents paleorecharge. The few available  $^{14}\text{C}$  data (Fig. 4) are consistent with that interpretation. The point ( $-11.2$ ,  $-77\text{\textperthousand}$ ) corresponds to mean winter precipitation on a north-facing slope in Chino Valley (Beisner et al., 2016). Similar mean winter precipitation and corresponding recharge appear to prevail throughout Area AZ-1, independent of altitude (Eastoe and Towne, 2018).

#### 4.3. Area HT, Hueco Bolsón-Tularosa Valley-Sacramento Mts., New Mexico, Texas, Chihuahua

Data are available for the alluvial basin-fill aquifers in the Hueco Bolsón (Dadakis, 2004; Eastoe et al., 2008, 2016) and for Tularosa Valley and a limestone aquifer in adjacent parts of the Sacramento Mts. (Eastoe and Rodney, 2014, sampling in 2003). An additional dataset for the Sacramento Mts (Newton et al., 2012, sampling in 2006–2009) has not been used, because stable isotope data indicated that heavy summer rains during the study period had rapidly recharged the limestone aquifer, strongly shifting values of  $\delta^{18}\text{O}$  and  $\delta^2\text{H}$  towards those of mean precipitation for the seasons immediately before sampling. The 2003 dataset appeared to represent long-term recharge in both the limestone and alluvial aquifers (see discussion in Eastoe and Rodney, 2014). Runoff from the Sacramento Mts. supplies water to the alluvial aquifer in Tularosa Valley, where several large canyons converge near Alamogordo. Samples with pMC  $>10$  define a linear trend, the Sacramento Mts. trend, SMT, with slope near 6 (Fig. 5a), controlled mainly by evaporation that is thought to occur as infiltration takes place through thick soil profiles in broad montane valleys (Eastoe and Rodney, 2014). The SMT originates in mean winter precipitation at the range crest, represented in Fig. 5a by bulk precipitation for December–March, collected at 2805 masl in 2007 and 2008 (Newton et al., 2012). Two samples from basin alluvium 56 and 105 km south of Alamogordo have

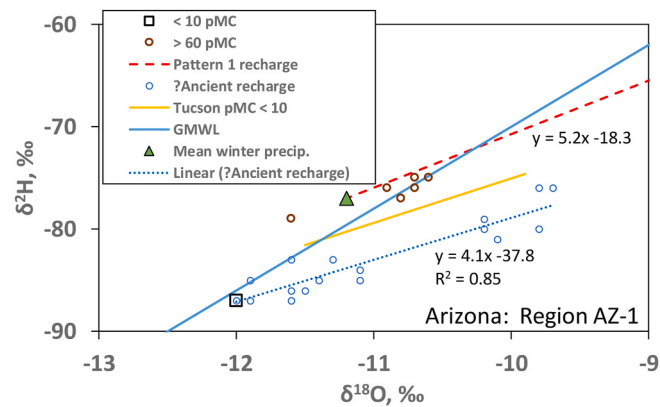
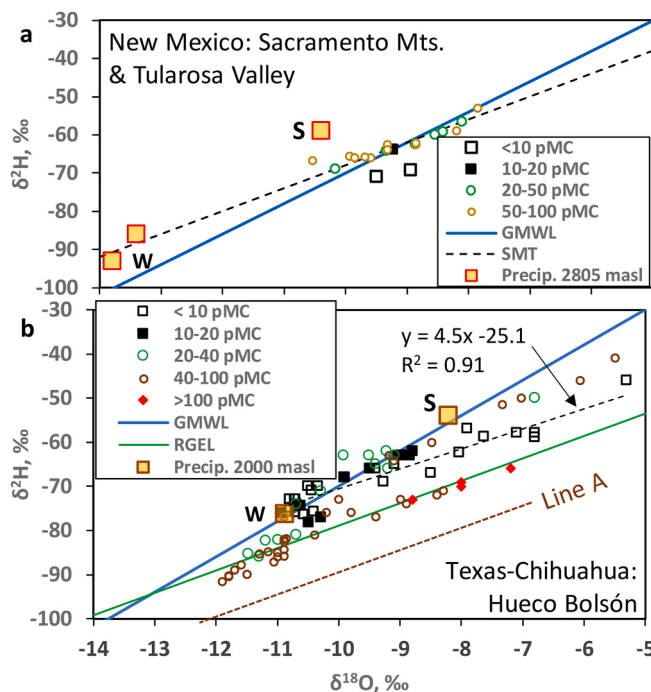


Fig. 4.  $\delta^2\text{H}$  vs.  $\delta^{18}\text{O}$  for Region AZ-1. Groundwater data with radiocarbon measurements are from Wirt and DeWitt (2005) and Eastoe (2007). Data for suspected ancient water, the linear trend for Pattern 1 recharge and mean winter precipitation in region AZ-1 are from Eastoe and Towne (2018). The linear trend for Tucson Basin, pMC  $<10$ , is from Fig. 3.



**Fig. 5.**  $\delta^2\text{H}$  vs.  $\delta^{18}\text{O}$  for Region HT, showing groundwater data with radio-carbon measurements. a. Sacramento Mountains and Tularosa Valley. Groundwater data and Sacramento Mountains trend (SMT) are from Eastoe and Rodney (2014). Precipitation means for 2805 masl (2007–2008) are from Newton et al. (2012). b. Hueco Bolsón. Groundwater data are from Dadakis (2004), Eastoe et al. (2008) and Eastoe et al. (2016); Rio Grande evaporation line (RGEL) is from Phillips et al. (2003). Precipitation means for 2000 masl, weighted for amount, are for the wettest 30% of months in Tucson Basin (Eastoe and Towne, 2018). W = winter, S = summer. Line A is explained in Section 4.6.

pMC <10 and appear to belong to a separate evaporation trend beneath the SMT.

In the Hueco Bolsón (Fig. 5b), groundwater originates either as recharge from the Rio Grande, identified by its association with the Rio Grande evaporation line (RGEL, data of Phillips et al., 2003) or as recharge of native basin water associated with the GMWL or with poorly defined evaporation trends above the RGEL (Eastoe et al., 2008). All samples plotting on the RGEL have pMC >20. Among native groundwaters, samples with pMC <10 define a broad evaporation trend with slope near 5 and an intercept on the GMWL at  $-11 < \delta^{18}\text{O} < -10\text{\textperthousand}$ , while most samples with pMC >10 have values of  $\delta^{18}\text{O}$  and  $\delta^2\text{H}$  close to the GMWL or on other evaporation trends. Native fresh groundwater on the western side of the Hueco Bolsón originates in the Organ Mts., 55 km north of El Paso (Hibbs et al., 1997), and salty water in the basin center probably originates in the Sacramento Mountains in Tularosa Valley (Druhan et al., 2008). No long-term isotope data are available for precipitation in this area; the mean compositions for winter and summer (Fig. 5b) are calculated from Tucson Basin data (Eastoe and Dettman, 2016) for the wettest 30% of months during which recharge mostly occurs (Eastoe and Towne, 2018). Altitude is adjusted to 2000 masl (corresponding to the Organ Mountains) using lapse rates from Eastoe and Wright (2019). If the comparison is valid, samples with pMC >10 represent Pattern 2 recharge, while samples with pMC <10 correspond to Pattern 1 recharge that originated as winter paleoprecipitation. Similar evolution occurs in area AZ-2 (Fig. 2). In the Hueco Bolsón, there appears to be little or no shift in the origin-point of the ancient evaporation trend relative to present-day winter precipitation.

#### 4.4. Area CH, Chihuahua

Data for alluvial aquifers near Ciudad Chihuahua (Mahlknecht et al., 2008) form a broad evaporation trend, which is compared in Fig. 6 with seasonal mean precipitation in Ciudad Chihuahua, 1962–1988 (International Atomic Energy Agency, 2022). The evaporation trend originates in winter precipitation, possibly as a combination of recharge from bulk precipitation with recharge from the largest events. Winter precipitation for 1962–1988 made up only 22% of the total precipitation for the period. Data for Indian Hot Springs (Table 2), which discharge from hard rock near the Rio Grande, appear to fall on the same evaporation trend, although two samples with <2 pMC may lie on a slightly lower evaporation trend. In both areas, recharge has about the same isotope composition regardless of  $^{14}\text{C}$  activity (except possibly for the two samples with pMC <2), and samples having pMC >100 are the most evaporated.

#### 4.5. Area EB-HP, Eastern Basins of the Cordillera and the High Plains, Texas, New Mexico

Data are available for Eagle Flat (Fig. 7a; data of Darling, 1997), an intermontane alluvial basin about 50 km west of a low-relief segment of the Cordilleran range front, and the Ogallala aquifer (Fig. 7b; data of Dutton, 1995) in Neogene siliciclastic strata of the High Plains immediately east of the range front. Values of  $\delta^{18}\text{O}$  and  $\delta^2\text{H}$  fall close to or left of the GMWL. Those with high  $^{14}\text{C}$  activity have high values of  $\delta^{18}\text{O}$  and  $\delta^2\text{H}$ , and overlap the upper ends of the ranges for samples with pMC <10. Samples with <10 pMC have broad ranges of  $\delta^{18}\text{O}$ : 2.6‰ at Eagle Flat, and 4.5‰ in the Ogallala aquifer.

To these may be added information from carbonate strata of the Delaware Basin (Fig. 7b; data of Lambert and Harvey, 1987), where relatively few  $^{14}\text{C}$  data were available. Groundwater in the Permian Rustler Formation was identified as “recent” or “ancient” according to whether it occurs near or far from recharge zones; a few of the “recent” category contained finite tritium, and one of the “ancient” group contained 3.7 pMC. “Ancient” waters define a field separate from and below the field of “recent” waters. Mixing with connate water may explain

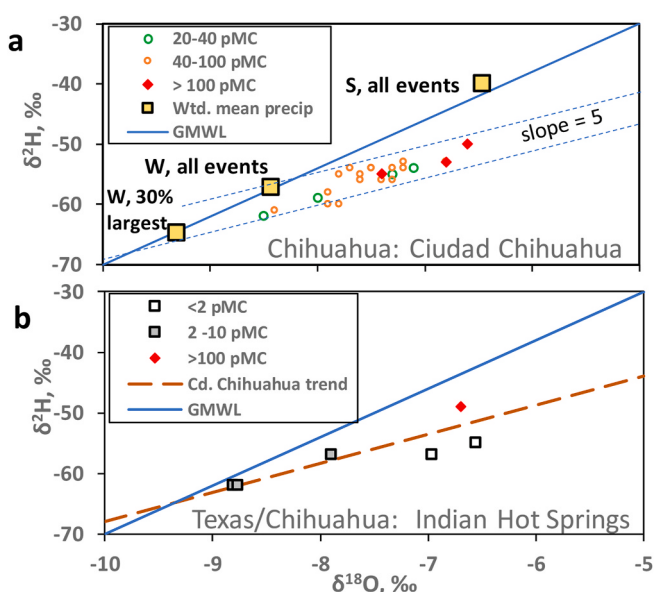


**Fig. 6.**  $\delta^2\text{H}$  vs.  $\delta^{18}\text{O}$  for Region CH, showing groundwater data with radio-carbon measurements. a. Ciudad Chihuahua, from Mahlknecht et al. (2008), and precipitation means from International Atomic Energy Agency (2022). Dashed lines are suggested evaporation trends of slope 5. b. Indian Hot Springs, data from Table 2. The Ciudad Chihuahua trend represents the groundwater data in Fig. 6a.

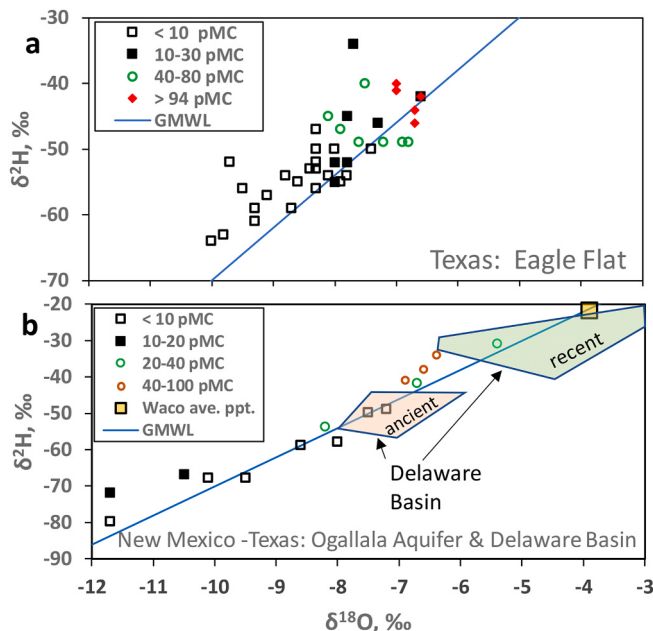


**Fig. 7.**  $\delta^2\text{H}$  vs.  $\delta^{18}\text{O}$  for Region EB-HP, showing groundwater data with radiocarbon measurements. a. Eagle Flat, data from Darling (1997). b. Ogallala aquifer, data from Dutton (1995) and Delaware Basin, data of Lambert and Harvey (1987) shown as colored fields established from geological criteria and a few radiocarbon data. Mean precipitation data for Waco, Texas, from International Atomic Energy Agency (2022).

samples plotting to the right of the GMWL.

#### 4.6. Area RGV, Rio Grande Valley, Colorado, New Mexico

In its upper reaches, the Rio Grande flows from the San Juan Mountains of Southern Colorado into the San Luis Basin (SLB), a broad rift filled with alluvium. Mayo et al. (2006) tabulated an extensive set of values of  $\delta^{18}\text{O}$ ,  $\delta^2\text{H}$  and  $^{14}\text{C}$  activity for confined groundwater and springs in the SLB. Confined groundwater was sampled from wells as deep as 1280 m, and most samples were from depths of 300–700 m. Samples with <10 pMC (Fig. 8a) have values of  $\delta^{18}\text{O}$  and  $\delta^2\text{H}$  near those of the GMWL and span three  $\delta^{18}\text{O}$  units; they largely overlap groundwater with 10 to >100 pMC. The pattern resembles that of confined groundwater in the San Pedro Valley (Section 4.1) and on the Colorado Plateau (Section 4.7). Altitude effects probably do not explain the range of  $\delta^{18}\text{O}$  values, but a paleoclimate effect may do so (Mayo et al., 2006). Samples with pMC <10 are divided into groups A and B in Fig. 8a. Group A has  $\delta^{18}\text{O} \leq -15.9\text{‰}$  and includes groundwater from the confined aquifers in what may be a stagnant volume midway between the Saguache River and the Rio Grande. Group B, which has  $\delta^{18}\text{O} \geq -15.7\text{‰}$ , includes two samples from hot springs. Waters of different flow path and residence time may therefore be involved. Group B plots close to the source composition of the present-day Rio Grande evaporation line (RGEL) of Phillips et al. (2003). Both A and B include samples with <2 pMC.

Data for Albuquerque Basin, 350 km downstream of SLB, are from Plummer et al. (2004). In the central parts of the basin, where recharge is from the Rio Grande, groundwater with <10 pMC forms a linear mixing trend (Fig. 8b) between water corresponding with group A in Fig. 8a and evaporated water like that in the present-day Rio Grande in Albuquerque (Phillips et al., 2003) with a source composition corresponding to group B in Fig. 8a. Water with pMC >20 plots between this trend and the RGEL, which has had its present form since the time represented by Group B data. No relationships between  $\delta^{18}\text{O}$ ,  $\delta^2\text{H}$  and  $^{14}\text{C}$  activity are present in groundwater from the eastern and western

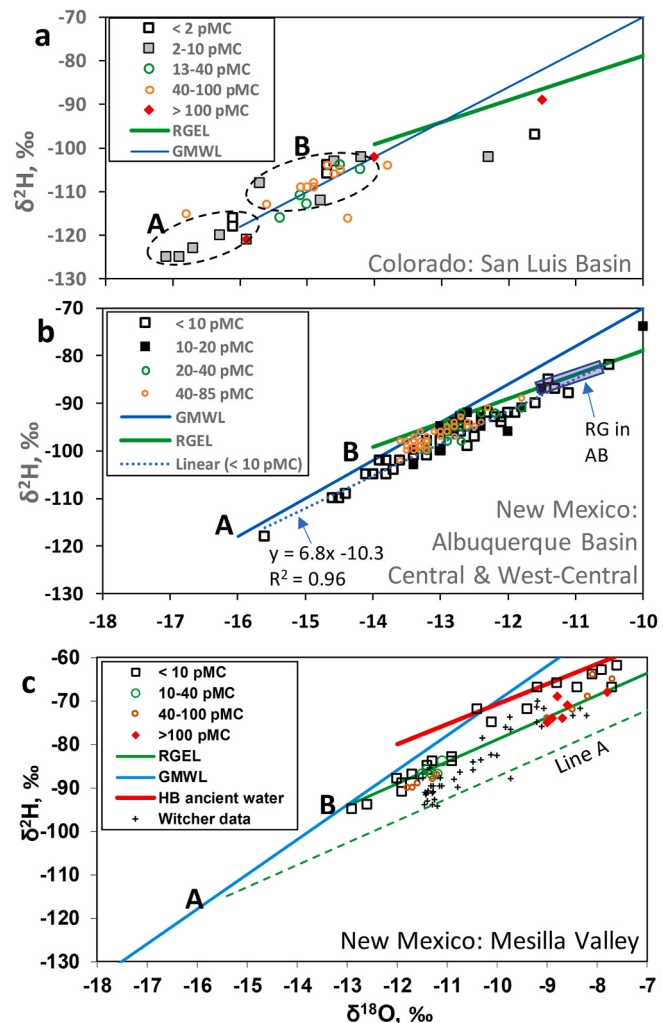


**Fig. 8.**  $\delta^2\text{H}$  vs.  $\delta^{18}\text{O}$  for Region RGV, showing groundwater data with radiocarbon measurements. RGEL = Rio Grande evaporation line, from Phillips et al. (2003). a. San Luis Basin, data of Mayo et al. (2006). b. Albuquerque Basin, the central and west central parts affected by recharge from the Rio Grande, data of Plummer et al. (2004). Data for other parts of Albuquerque basin are shown in Supplementary Fig. S2. The field "RG in AB" shows the present-day range of Rio Grande surface water in Albuquerque Basin (Phillips et al., 2003). Points A and B are present-day and ancient Rio Grande surface water without evaporation (compare Fig. 8a). c. Mesilla Valley, data of Nickerson (2006) along with  $\delta^2\text{H}$  and  $\delta^{18}\text{O}$  data (without  $^{14}\text{C}$  measurements) from Witcher et al. (2004). HB ancient water is the trend of groundwater data with pMC <10 in the neighboring Hueco Bolsón, taken from Fig. 5b. Points A and B as in Fig. 8b, with a suggested ancient evaporation trend (green dashes) originating at point A.

flanks of Albuquerque Basin (Supplementary Fig. S2), possibly because of mixing between local and river recharge.

Data for Mesilla Valley, 750 km downstream of SLB, are from Teeple (2017) and Nickerson (2006). The data confirm that the present RGEL (originating at B) was established by the time represented by samples with pMC <10. None of these samples plots near line A, a proposed evaporation trend originating in group A of Fig. 8a. However,  $\delta^{18}\text{O}$  and  $\delta^2\text{H}$  measurements without accompanying radiocarbon data for several deep-basin groundwater samples (Witcher et al., 2004) indicate mixing between line A and the RGEL, like that in Albuquerque Basin but with higher degrees of evaporation in both end members. Native groundwater (not recharged from the Rio Grande) like that with pMC <10 in the neighboring Hueco Bolsón, is present in Mesilla Valley, and such waters have mixed with recharge from the Rio Grande.

In the Hueco Bolsón, 800 km downstream of SLB, no samples with

pMC <10, corresponding with ancient groups A and B water from SLB, have been identified (Fig. 5b).

#### 4.7. Area CP, Colorado Plateau, Arizona, New Mexico

Groundwater samples are from porous strata of the Colorado Plateau: the N-aquifer in the Jurassic Navajo Sandstone in northeastern Arizona (Lopes and Hoffman, 1997; Zhu, 2000), the Cretaceous-Paleogene Ojo Alamo and Nacimiento aquifers of the San Juan Basin, New Mexico (Phillips et al., 1986), the Permian Coconino Sandstone (C-aquifer) and Mississippian carbonate aquifers of the Mogollon Rim near Flagstaff and Payson, Arizona (Bills et al., 2000; Wirt and DeWitt, 2005; Eastoe 2007) and Neogene volcanic rocks of the Pajarito Plateau, New Mexico (Longmire et al., 2007). Surface relief of terrain likely to contribute to recharge varies relatively little within the first two areas. The last two areas are adjacent to volcanic peaks with elevations of 3000–4000 masl.

The N-aquifer data (Fig. 9a) with pMC <10 are similar to those in the SLB (Section 4.6), and have a  $\delta^{18}\text{O}$  range of -13 to <-16‰, projected on to the GMWL using an evaporation trend of slope 5. At the lower end of the range, the waters are evaporated. At the upper end, the waters show little isotope evidence of evaporation and correspond to the source water for a broad evaporation trend containing most samples with pMC >20. The data pattern for the San Juan Basin (Fig. 9b) is similar, but less clear; the source water for samples with pMC >20 corresponds to present-day surface water in the San Juan River (Coplen and Kendall, 2000).

At the Mogollon Rim near Flagstaff, Arizona (Fig. 9c), data with pMC >20 have values of  $\delta^{18}\text{O}$  and  $\delta^2\text{H}$  close to winter-precipitation means calculated from data for Payson and Flagstaff, Arizona (Table 2; Beisner et al., 2016; International Atomic Energy Agency, 2022), but far from summer means. Two data points with pMC <20 have values of  $\delta^{18}\text{O}$  and  $\delta^2\text{H}$  higher than those of Flagstaff winter precipitation. No data with pMC <20 were measured for the Pajarito Plateau (Fig. 9d); data with pMC >100 mainly have  $\delta^{18}\text{O}$  and  $\delta^2\text{H}$  values less than those of other

samples. No clear relationships between  $^{14}\text{C}$  activity,  $\delta^{18}\text{O}$  and  $\delta^2\text{H}$  exist at the Mogollon Rim and Pajarito Plateau.

#### 4.8. Area NV, southern Nevada

Data are available from the regional alluvial and carbonate aquifers of the southern Great Basin extending from Pahranagat Valley through the Nevada Test Site to the Amargosa Desert and south to Las Vegas Valley (Winograd and Pearson, 1976; Rose et al., 1997; Thomas et al., 1996) and for a fractured-rock aquifer at Yucca Mountain (Yang et al., 1996). In the southern Great Basin, samples with pMC <10 span a broad range of  $\delta^{18}\text{O}$  and  $\delta^2\text{H}$ , as in SLB and Colorado Plateau aquifers (Sections 4.6, 4.7), and overlap data for samples with 20–100 pMC (Fig. 10a, b, c). Most samples with pMC >100 have lower values of  $\delta^{18}\text{O}$  and  $\delta^2\text{H}$  than other samples (Fig. 10a). A small dataset for Pahranagat Valley shows a distinction between samples with pMC <10 (low  $\delta^{18}\text{O}$  and  $\delta^2\text{H}$  values) and with pMC < between 70 and 100 (high  $\delta^{18}\text{O}$  and  $\delta^2\text{H}$  values), all values forming a single, scattered evaporation trend.

#### 4.9. Area SEC, southeastern California

In the part of the Mojave Desert flanking the San Bernardino Mountains, groundwater with pMC <10 in a regional confined aquifer has  $\delta^{18}\text{O}$  values < -11‰, in contrast with young (<100 years; no  $^{14}\text{C}$  activity data published) groundwater in overlying fluvial-alluvial deposits (Kulogoski et al., 2009). All data coincide with the GMWL. Data of Mathany et al. (2012) for alluvial aquifers in Borrego Valley, the Central Desert and “low-use basins” near the Colorado River show no relationships between  $\delta^{18}\text{O}$ ,  $\delta^2\text{H}$  and  $^{14}\text{C}$ . Data from both studies are shown in Supplementary Fig. S3.

#### 4.10. Area WC, West Coast

In Baja California Sur, data are available for an alluvial aquifer at La Paz (Tamez-Meléndez et al., 2016), and the geothermal field at Las Tres

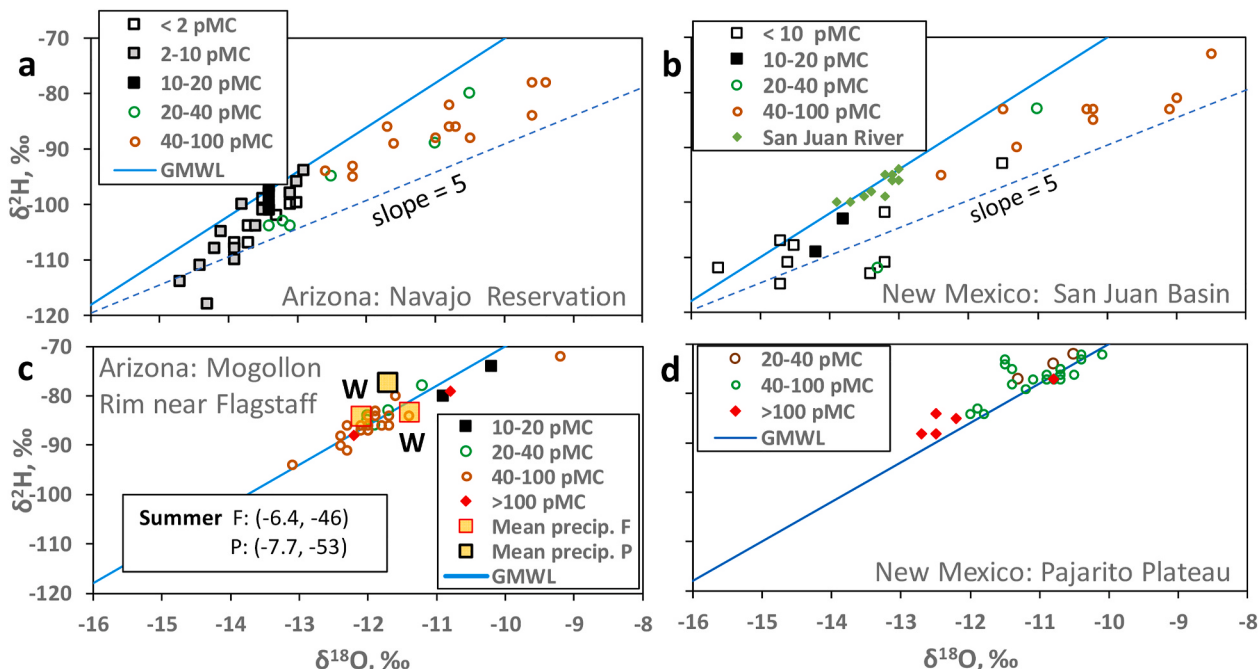


**Fig. 9.**  $\delta^2\text{H}$  vs.  $\delta^{18}\text{O}$  for Region CP, showing groundwater data with radiocarbon measurements. a. Navajo Reservation, data of Zhu (2000) and Lopes and Hoffman (1997). b. San Juan Basin, data for groundwater from Phillips et al. (1986), and for surface water from Coplen and Kendall (2000). c. The Mogollon Rim near Flagstaff, data for groundwater from Bills et al. (2000). Weighted seasonal means for precipitation at Flagstaff (F) are from International Atomic Energy Agency (2022), and at Payson, from Eastoe (2007). Winter means (W) are plotted; summer means fall outside the diagram and are listed in the inset. d. Pajarito Plateau, data of Longmire et al. (2007).

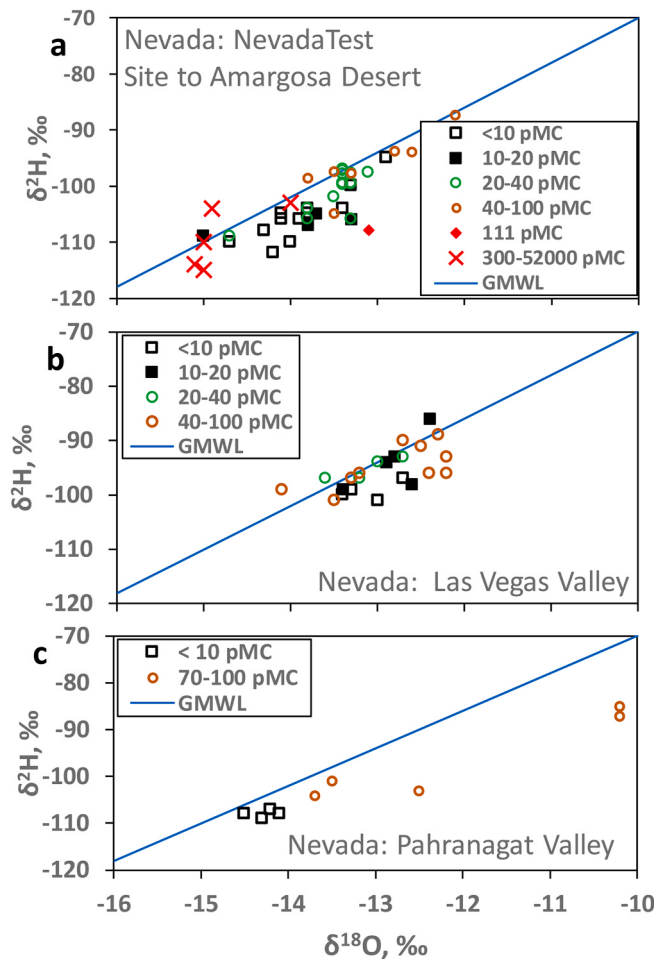


**Fig. 10.**  $\delta^2\text{H}$  vs.  $\delta^{18}\text{O}$  for Region NV, showing groundwater data with radiocarbon measurements, data of Thomas et al. (1996) and Rose et al. (1997). a. Nevada Test Site and Amargosa Desert. b. Las Vegas Valley. c. Pahranagat Valley.

Vírgenes volcanic edifice (Birkle et al., 2016). At La Paz (Fig. 11a), data lie along the GMWL, with  $^{14}\text{C}$  activity increasing downwards; no data with pMC <25 are reported. At Las Tres Vírgenes (Fig. 11b), a few  $^{14}\text{C}$  data are available for geothermal waters; four of five have pMC <20. These have the same range of  $\delta^2\text{H}$  as the lowest- $^{14}\text{C}$  water at La Paz but  $\delta^{18}\text{O}$  values are shifted to the right because of oxygen-isotope exchange with hot rock. Assuming shallow, cool groundwater to be younger than deep, geothermal water, the pattern is similar to that at La Paz, with  $^{14}\text{C}$  activity increasing as  $\delta^2\text{H}$  decreases.

In Los Angeles Basin, California, ( $\delta^{18}\text{O}$ ,  $\delta^2\text{H}$ ) pairs of samples unaffected by imported water lie on the GMWL (Figure 16 of Reichard et al., 2003). A plot of  $\delta^2\text{H}$  vs. pMC (Fig. 11c) is used here because  $\delta^{18}\text{O}$  values cannot be linked with  $^{14}\text{C}$  activity in the report. West of the Los Angeles River, where recharge originates as low-elevation precipitation, ranges of  $\delta^2\text{H}$  are -41 to -53‰ for pMC >8 and -51 to -63‰ for pMC <8. A positive shift of about 12‰ in  $\delta^2\text{H}$  (corresponding to 1.5‰ in  $\delta^{18}\text{O}$ ) has occurred since the time represented by pMC values between 5 and 8. The shift cannot be seen in the eastern part of the basin, where  $\delta^2\text{H}$  in recharge is affected by runoff from high-elevation mountains to the north.

#### 4.11. Area CRD, Colorado River Delta, Sonora, Baja California

Data from Birkle et al. (2016) and Zamora et al. (2019, 2021) show no recognizable relationships between  $\delta^{18}\text{O}$ ,  $\delta^2\text{H}$  and  $^{14}\text{C}$  activity (Supplementary Fig. S4).

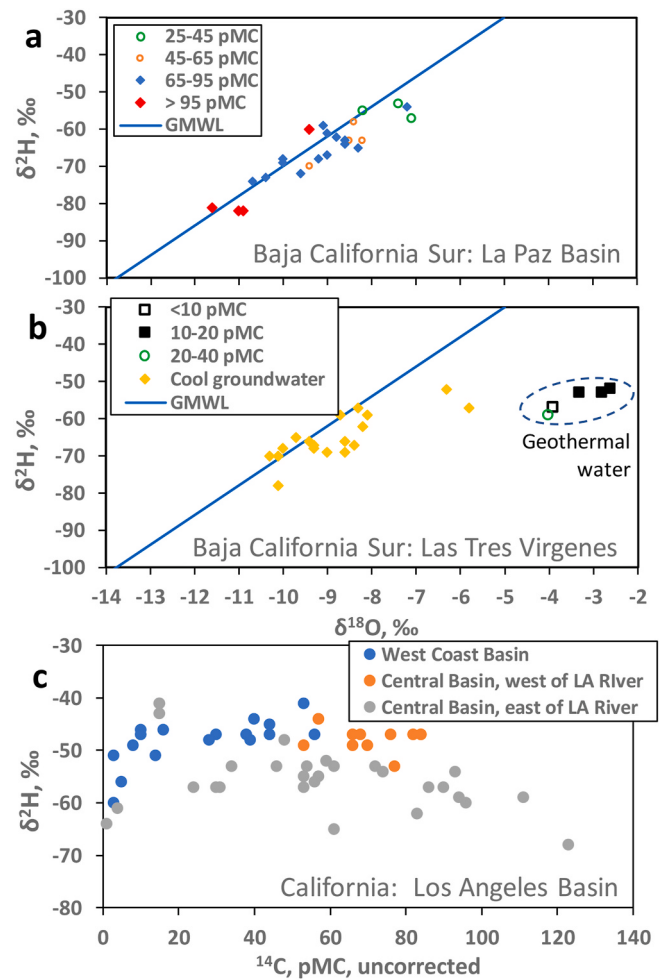


**Fig. 11.**  $\delta^2\text{H}$  vs.  $\delta^{18}\text{O}$  for Region WC, showing groundwater data with radiocarbon measurements. a. La Paz Basin, data of Tamez-Meléndez et al. (2016). b. Las Tres Vírgenes geothermal field, data of Birkle et al. (2016), including stable isotope measurements without  $^{14}\text{C}$  measurements for cool groundwater. c. Los Angeles (LA) Basin,  $\delta^2\text{H}$  vs. pMC, data of Reichard et al. (2003).

#### 4.12. Abundance of fossil water

Table 3 shows the frequency of occurrence of groundwater containing <10 pMC in the study area, for those datasets comprising 25 or more  $^{14}\text{C}$  measurements. For this criterion, the range of fossil water occurrence is 0–56%, considering basins individually. Aggregated data for all twelve basins in Table 3 include 24% fossil water.

### 5. Discussion

#### 5.1. Evaluation of approach

In Area AZ-2, 10 pMC, without correction, functions as a threshold for identifying groundwater old enough to show climate-related stable isotope effects near the end of the Pleistocene. Results for groundwater with 10–20 pMC are equivocal; some results are the same as the group containing <10 pMC and others are not (Fig. 2). In cases with enough data (e.g. Figs. 8a and 9a), use of a lower  $^{14}\text{C}$  activity threshold results in no additional separation of the stable isotope data. However, in La Paz (Baja California Sur), groundwater with 25–45 pMC is isotopically distinctive from younger groundwater, and in Los Angeles Basin (California), the threshold is 5–8 pMC.

The relationship between 10 pMC as a threshold and stable isotopes applies in numerous areas of southwestern North America, but not in

**Table 3**  
Frequency of Occurrence of Samples with <10 pMC

Basin	State	Depth range*	Aquifer	No. of pMC measured	No. with <10 pMC	% <10 pMC	Data source
		m	material				
Albuquerque	New Mexico	600	alluvium	195	47	24	Plummer et al. (2004)
Hueco Bolson	Texas/Chihuahua	350	alluvium	88	23	26	Eastoe et al. (2008, 2016); Eastoe and Rodney (2014)
Tucson	Arizona	300	alluvium	82	3	4	Eastoe et al. (2004)
San Pedro	Arizona	300	alluvium	60	4	7	Baillie et al. (2007); Hopkins et al. (2014)
Los Angeles	California	400	alluvium	59	6	10	Reichard et al. (2003)
Navajo Sandstone (Colorado Plateau)	Arizona	300	sandstone	47	23	49	Zhu (2000)
Eagle Flat	Texas	300	alluvium + hard rock	45	24	56	Darling (1997)
Nevada Test Site basins	Nevada	?	alluvium + hard rock	45	15	33	Thomas et al. (1996); Lopes and Hoffman (1997)
Mesilla	New Mexico	<600	alluvium	41	21	51	Teeple (2017)
San Luis	Colorado	1200	alluvium	36	16	44	Mayo et al. (2006)
Pajarito Plateau	New Mexico	<500	tuff/fanglomerate	30	0	0	Longmire et al. (2007)
La Paz	Baja California Sur	200	alluvium	25	0	0	Tamez-Meléndez et al. (2016)
All data				753	182	24	

every case. In four instances, San Pedro Valley (Fig. 2c) San Luis Basin (Fig. 8a), the Navajo Reservation (Fig. 9a) and San Juan Basin (Fig. 9b), some groundwater with <10 pMC has distinctive values of  $\delta^{18}\text{O}$  and  $\delta^2\text{H}$ , while other measurements overlap the data for younger groundwater. All four basins contain deep, confined groundwater, some of which has pMC <2. Broad ranges of  $\delta^{18}\text{O}$  and  $\delta^2\text{H}$  for samples with <10 pMC are also present in Eagle Flat (Fig. 7a), and the Ogallala Aquifer (Fig. 7b). In these cases, values of  $\delta^{18}\text{O}$  and  $\delta^2\text{H}$  lie near the GMWL and distinguish water with <10 pMC from younger water. These six basins may preserve water from two or more different climate regimes in the late Pleistocene.

## 5.2. Chronology

The timing of the latest increase in  $\delta^{18}\text{O}$  of precipitation is constrained by dated speleothems at 13–15 ka in southern Arizona (Wagner et al., 2010), and about 15 ka in southeastern New Mexico (Asmerom et al., 2010). The 10 pMC threshold value used here corresponds to a positive shift, mainly 1–2‰ in  $\delta^{18}\text{O}$ , of groundwater in several basins of the study area. The  $\delta^{18}\text{O}$  shift in groundwater is identified as the attenuated output signal corresponding to the 2–3‰ input signal in the speleothems.

As noted above, pre-15 ka precipitation with values of  $\delta^{18}\text{O}$  and  $\delta^2\text{H}$  like those of present-day precipitation survives as groundwater in deep, confined portions of certain basins. In speleothem calcite, values of  $\delta^{18}\text{O}$  overlapping those of material deposited since 13–15 ka are found at 54–55 ka in southeastern New Mexico (Asmerom et al., 2010) and 51–53 ka in southern Arizona (Wagner et al., 2010), but not in intervening speleothem bands. Some ancient groundwater therefore appears to have been resident in more stagnant parts of the basins studied here for >51 ka. Mixing trends of this water with younger groundwater that has pMC <10 are present in data from San Luis Basin (Fig. 8a), Eagle Flat (Fig. 7a) and the Ogalalla Aquifer (Fig. 7b).

## 5.3. Additional complicating factors

Evidence for positive temporal shifts in  $\delta^{18}\text{O}$  and  $\delta^2\text{H}$  of precipitation across the southwestern USA from the California coast to the High Plains of New Mexico appears to indicate a regional climate phenomenon at 13–15 ka. Exceptions with a confused relationship between  $^{14}\text{C}$  and stable isotopes therefore most likely reflect local complicating factors. In basins with large altitude differences between well-watered mountain

summits and arid or semiarid basin floors, present-day isotope altitude effects may provide an alternative mechanism of generating low  $\delta^{18}\text{O}$  and  $\delta^2\text{H}$  values that may overlap those of paleorecharge. Altitude effects may explain the confused relationships between  $\delta^{18}\text{O}$  and  $^{14}\text{C}$  in basins with large altitude ranges, e.g., Las Vegas Valley, (Fig. 10b; altitude range ~2600 m), on the Mogollon Rim (Fig. 9c; range ~1600 m), in Borrego Valley and the Central Desert, California (Supp. Figure 3c, ranges ~1600 m) and on the eastern flanks of Albuquerque Basin, New Mexico (Supp. Fig. S2, range ~1200 m). In the area around Tucson, Arizona, the separation between groundwater with <10 pMC and younger groundwater is clearer in the Santa Rita and Patagonia Mountains (Fig. 2b, local range <700 m) than in Tucson Basin (Fig. 2a; range ~2000 m). Another example occurs in Los Angeles basin, California (Fig. 11c), where groundwater west of the Los Angeles River (range <400 m) shows a clearer relationship between  $\delta^2\text{H}$  and  $^{14}\text{C}$  activity than groundwater east of the Los Angeles River (range 1400 m).

The sources of recharge and subsequent mixing of groundwater at the Nevada Test Site (NTS) are potentially complicated by very long groundwater flow paths combined with interbasin flow, both at a scale of 100–200 km (Winograd and Pearson, 1976; Davisson et al., 1999); under such conditions heterogeneous flow may confuse relationships between  $^{14}\text{C}$  activity and stable isotopes (Fig. 10a). An alternative possibility is that no pre-bomb temporal isotope shift exists in this area, as suggested by the small dataset for Pahranagat Valley where evaporation of a single source composition can account for the data array (Section 5.7).

A more likely confounding factor at the NTS is anthropogenic  $^{14}\text{C}$ . In most of the northern hemisphere,  $^{14}\text{C}$  activity in groundwater as a result of natural recharge is limited to a value less than 180 pMC, the annual average in the atmosphere at the peak of atmospheric nuclear testing (e.g., Burchuladze et al., 1989). Contamination from nuclear testing has occurred at the NTS, where some groundwater has  $^{14}\text{C}$  activities of 300–52000 pMC (Rose et al., 1997). It is also likely at Pajarito Plateau, New Mexico (Fig. 9d) where 194 pMC was measured in groundwater from a canyon into which tritium-bearing reactor effluent from the Los Alamos National Laboratory was discharged between 1943 and 1964 (Longmire et al., 2007). Lesser degrees of contamination are likely in some samples with <100 pMC in both areas, providing an alternative explanation for the confused relationships between  $^{14}\text{C}$  activity and stable isotopes.

Delayed melting of glacial ice may juxtapose values  $\delta^{18}\text{O}$  and  $\delta^2\text{H}$  in ancient precipitation with younger apparent  $^{14}\text{C}$  ages set at the time of

infiltration of meltwater runoff. In the Qilian Mountains, Gansu, China, large differences in  $\delta^{18}\text{O}$  and  $\delta^2\text{H}$  of precipitation in the past ~20 ka are recorded in groundwater, and continue to affect the stable isotope composition of runoff from high elevations (Zhao et al., 2018; Xie et al., 2022). A confused relationship between  $^{14}\text{C}$  activity and stable isotopes in piedmont alluvial aquifers recharged from the Qilian Mountains (Jiang et al., 2019) is probably related to delayed ice melting. Pleistocene glaciers, present in central and northern Nevada, the San Francisco Peaks of Arizona and the San Juan Mts. of Colorado (Osborn, 2004; Laabs et al., 2013) may have contributed meltwater to the NTS, the Mogollon Rim near Flagstaff and the San Luis Basin.

In the Colorado River delta, stable isotope data patterns are complicated by differing degrees of evaporation in the river, along with mixing between river water and local recharge (Zamora et al., 2021). Changes in degree of evaporation over time (high evaporation during the latest Pleistocene and at present; lower evaporation at other times) also appear in the Rio Grande basin (Fig. 8b).

#### 5.4. A post-bomb isotope shift?

Unexplained groups of samples with >100 pMC and with low values of  $\delta^{18}\text{O}$  and  $\delta^2\text{H}$  occur in two areas. At the NTS (Fig. 10a), all six samples with >100 pMC have values of  $\delta^{18}\text{O}$  and  $\delta^2\text{H}$  similar to or lower than those of samples having <10 pMC. On Pajarito Plateau (Fig. 9d), four of five samples with >100 pMC have lower values of  $\delta^{18}\text{O}$  and  $\delta^2\text{H}$  than samples with <100 pMC. Underground contamination with  $^{14}\text{C}$  is unlikely to have affected only groundwater with limited ranges of  $\delta^{18}\text{O}$  and  $\delta^2\text{H}$ . Rather, recharge following a negative shift in  $\delta^{18}\text{O}$  and  $\delta^2\text{H}$  of precipitation occurred during the bomb-spike in atmospheric  $^{14}\text{C}$ . The source of  $^{14}\text{C}$  may have been global or local; in either case the high  $^{14}\text{C}$  measurements indicate that the negative shift in  $\delta^{18}\text{O}$  and  $\delta^2\text{H}$  occurred since 1953. Clear evidence of the shift is seen only in the northern part of the study area, and only where enough samples with pMC >100 are available.

A human cause for the negative shift in  $\delta^{18}\text{O}$  and  $\delta^2\text{H}$  is possible. Lo and Famiglietti (2013) proposed that evaporation of irrigation water from the Central Valley of California increases the amount of summer rainfall in the continental interior to the east. Large deliveries of irrigation water to the Central Valley have occurred since the early 1970s; demand is greatest between May and July, but deliveries also take place between October and December (Galloway and Riley, 2006; Faunt et al., 2009, Figure C23). Deliveries come from the Sacramento River and streams draining the Sierra Nevada, and are locally supplemented with deep, confined paleowater from the Central Valley. Such water has  $\delta^{18}\text{O}$  between -9 and -15‰ (Coplen and Kendall, 2000; Davis and Coplen, 1989), in contrast with native groundwater in which  $\delta^{18}\text{O} > -9\text{\textperthousand}$  (e.g., Davis and Coplen, 1989; Davission and Criss, 1993). Vapor with low  $\delta^{18}\text{O}$  may therefore be advected inland from the Central Valley during much of the year as a result of water deliveries for irrigation, combined with lagged evapotranspiration (ET). The initiation of large surface water deliveries to the Central Valley in the early 1970s is consistent with the post-bomb appearance of low-  $\delta^{18}\text{O}$  rain in Nevada and New Mexico.

In the case of Pajarito Plateau, low-  $\delta^{18}\text{O}$  vapor may have advected from Lake Powell, filled during the 1960s. The reservoir accumulates Colorado River inflow with  $\delta^{18}\text{O} < -15.5\text{\textperthousand}$  (Guay et al., 2006).

#### 5.5. Effects of known climate change at 13–15 ka on groundwater

Fig. 12a depicts schematically the types of shift in  $\delta^{18}\text{O}$  and  $\delta^2\text{H}$  between groundwater samples with <10 pMC and younger samples in the study area. The spatial distribution of each type is shown in Fig. 12b, and basins with broad ranges of  $\delta^{18}\text{O}$  and  $\delta^2\text{H}$  in ancient water (Section 5.1) are indicated.

Patterns 1 and 2, the regional recharge mechanisms described in Arizona (see Section 2) appear to reflect the influence of climate on ET. In area AZ-1 where Pattern 1 prevails, ET prevents summer recharge

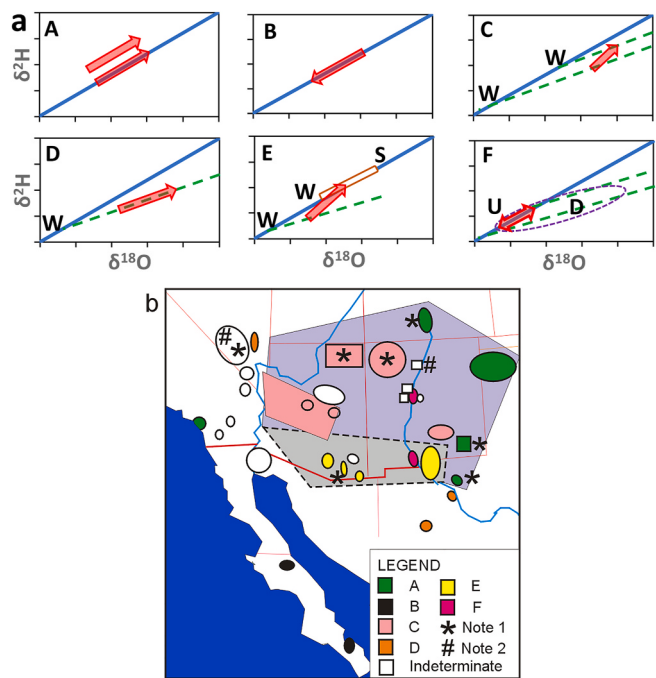


**Fig. 12.** a. Schematic plots of  $\delta^2\text{H}$  vs.  $\delta^{18}\text{O}$  showing identified patterns of stable isotope data in relation to measured  $^{14}\text{C}$  activity expressed as pMC. A: positive shift with increasing  $^{14}\text{C}$  activity, on or above GMWL; B: negative shift with increasing  $^{14}\text{C}$  activity; C: positive shift with increasing  $^{14}\text{C}$  activity, strong evaporation; D: no shift with increasing  $^{14}\text{C}$  activity, degree of evaporation increasing with time; E: positive shift with increasing  $^{14}\text{C}$  activity, accompanied by shift from pattern 2 to pattern 1 recharge; F: in Rio Grande basins, positive shift with increasing  $^{14}\text{C}$  activity in upstream (U) basin governs shifts in downstream (D) basins, with increasing evaporation downstream. b. Map of southwestern North America (compare Fig. 1 for site names), showing the distribution of patterns of data from Fig. 12a. Note 1: sites with wide ranges of  $\delta^{18}\text{O}$  and  $\delta^2\text{H}$  in groundwater with pMC < 10, including some data overlapping those of samples with >10 pMC. Note 2: sites with anthropogenic  $^{14}\text{C}$  contamination. Purple polygon: winter-only recharge. Grey polygon: where Pattern 2 (winter + summer) recharge has supplanted Pattern1 (winter-only) recharge.

entirely, while in AZ-2 (Pattern 2), ET prevents recharge in both summer and winter, except during the wettest 30% (approximately) of months.

Pattern 2 recharge (type E of Fig. 12) has replaced Pattern 1 (types A and C) over a broad area, the grey polygon in Fig. 12b, in the core region of the North American monsoon (Douglas et al., 1993). Note that Eastoe and Towne (2018) provide many additional examples of Pattern 2 recharge in that area, but that these lack accompanying  $^{14}\text{C}$  data. Apparent exceptions are Mesilla Valley, New Mexico (Fig. 8c) and Safford Basin, Arizona (Fig. 2d). In Mesilla Valley, sampled groundwater originates mainly in the Rio Grande, for which  $\delta^{18}\text{O}$  and  $\delta^2\text{H}$  are controlled by climate phenomena in San Luis Basin, Colorado (Section 4.6). In Safford Basin, altitude effects and a very small  $^{14}\text{C}$  dataset preclude recognition of isotope patterns like those of the other basins. The movement of Pattern 2 recharge into the area where Pattern 1 formerly operated appears to represent a northward progression of climate phenomena, reflected in groundwater as a northward migration of summer recharge. Migration of Pattern 2 into basins of western Arizona appears to have continued after 13–15 ka (Eastoe and Towne, 2018).

Pattern 1 recharge (types A and C of Fig. 12a) occurs in the purple polygon of Fig. 12b. In this zone, predominant recharge has consistently derived from winter precipitation, and the 13–15 ka positive isotope shift is recorded. Degrees of evaporation vary in space and time.

### 5.6. Climate change in Baja California inferred from isotope data

A different evolution of recharge sources appears to occur in parts of Baja California. At present, precipitation in Baja California occurs predominantly during winter and spring as far south as the area labeled “southern Baja California State” in Fig. 13, except along the eastern coast of the peninsula (Hastings and Turner, 1965). Winter-spring precipitation also predominates in Los Angeles Basin, California (Table 1).

The higher values of  $\delta^{18}\text{O}$  ( $>-9\text{\textperthousand}$ ) and  $\delta^2\text{H}$  ( $>-60\text{\textperthousand}$ ) in Baja California groundwater resemble the recharge that occurs from winter-spring frontal rain in Los Angeles Basin (Reichard et al., 2003). Such values predominate in cool groundwater as far south as southern Baja California State (Kretzschmar and Frommen, 2003), except on the east coast of Baja California at San Felipe (Carreón-Díazconti et al., 2017). Such values also occur in the oldest groundwater (Section 4.10; Fig. 11) sampled at Las Tres Vírgenes (Birkle et al., 2016) and La Paz (Tamez-Meléndez et al., 2016).

The lower values of  $\delta^{18}\text{O}$  ( $-9.0$  to  $-11.6\text{\textperthousand}$ ) and  $\delta^2\text{H}$  ( $-60$  to  $-82\text{\textperthousand}$ ) at La Paz and Las Tres Vírgenes, Baja California Sur, resemble recharge from tropical cyclonic rain in late summer and autumn in recent decades (Eastoe et al., 2014). Similar values of  $\delta^{18}\text{O}$  and  $\delta^2\text{H}$  (averages  $-10.1$ ,  $-73\text{\textperthousand}$ , respectively) were recorded in autumn rain from tropical cyclonic weather systems between 2018 and 2021 at Loreto, Baja California Sur (González-Hita et al., 2021), where they contrast with precipitation from winter and monsoon weather systems (means  $-4.9\text{\textperthousand}$ ,  $-29\text{\textperthousand}$ ).

Fig. 13 shows the distribution of  $\delta^{18}\text{O}$  in groundwater of the region around Baja California (Ojeda, 1998; Kretzschmar and Frommen, 2003; Szynkiewicz et al., 2008; Wassenaar et al. (2009); Négrel and Petelet-Giraud, 2011; Neff (2015); Birkle et al. (2016); Tamez-Meléndez et al. (2016); Carreón-Díazconti et al., 2017; Ledesma Ruiz et al., 2017). Existing  $^{14}\text{C}$  data, in conjunction with  $\delta^{18}\text{O}$  and  $\delta^2\text{H}$ , imply that winter-spring recharge like that in Los Angeles Basin predominated as

far south as La Paz, Baja California Sur at times represented by 25–45 pMC at La Paz, and  $<30 \pm 10$  pMC at Las Tres Vírgenes. Such a change has not occurred on the coast of Sonora, even though much precipitation from tropical cyclonic depressions falls along the coast there. The negative shift of  $\delta^{18}\text{O}$  and  $\delta^2\text{H}$  in groundwater over time is the reverse of the positive shifts in Los Angeles and southern Arizona. A positive shift observed between geothermal and cool groundwater at Santo Thomas in Baja California state (Kretzschmar and Frommen, 2003) probably also represents the 13–15 ka isotope shift in precipitation. Climate has changed in Baja California by the northward progression of the zone of predominant tropical-cyclonic precipitation, absent at some time in the early Holocene at least as far south as La Paz, but currently dominating recharge in the areas with red symbols in Fig. 13.

### 5.7. Places with no isotope shift

At Ciudad Chihuahua (Fig. 6a), Indian Hot Springs (Fig. 6b) and Pahranganat Valley (Fig. 10c), stable isotope data form a single evaporation trend in each case, and no difference in source water (projecting the isotope data back to the GMWL) can be seen between samples with pMC  $<10$  and younger samples. Younger samples are more evaporated, indicating a shift towards hotter or drier climate, or both, since 13–15 ka. These datasets may be evidence of northwestern and southeastern boundaries to the area in which an isotope shift occurred at 13–15 ka.

### 5.8. Implications for water resources

The fossil water abundance statistics for southwestern North America (Section 4.12) may be compared with estimates from Jasechko et al. (2017) for a set of basins spanning the globe, with lower spatial density than in the present study. Within 300 m of the surface, Jasechko et al. (2017) estimated 22–74% of total storage was fossil water, and within 1000 m, 42–85%. The comparison is not precise because the stable-isotope threshold adopted here is 13–15 ka (assuming that speleothems date the late Pleistocene isotope shift) rather than 11.7 ka (assuming accurate corrected  $^{14}\text{C}$  measurements). Nonetheless, fossil groundwater appears to be much less common in the study area than in the global dataset of Jasechko et al. (2017). The difference may arise because most aquifers represented in Table 3 consist of Neogene, poorly consolidated alluvium through which groundwater is flushed rapidly. No consistent relationship appears to exist between the ranges of sampling depth and fraction of fossil water. Datasets for this study and Jasechko et al. (2017) come mainly from water-supply wells producing potable water. Most such wells produce from the first potable water encountered, biasing sampling towards shallower aquifers, and against deeper aquifers or high-salinity water that may include a larger fraction of fossil water.

Natural climate change since the beginning of the Holocene has been accompanied by changes in groundwater recharge seasonality in Baja California and in the core region of the North American monsoon. In the latter, recharge in both summer and winter has supplanted winter-only recharge. The changes in regime appear to have progressed northward in both areas. Elsewhere in the study area, climate change has caused increases in degree of evaporation of recharge. Human-caused climate change is likely to modify or accelerate such changes. In the context of groundwater modeling, the study indicates that present recharge mechanisms cannot be assumed for fossil groundwater.

### 5.9. Future research

#### 5.9.1. Conclusions and recommendations

The datasets examined in this study were originally interpreted in the contexts of individual basins or small sub-regions of the study area. Considered jointly at broad regional scale, the data provide new insights into the effects of late Pleistocene climate change on recharge mechanisms across the study area, and into localized Holocene climate change.

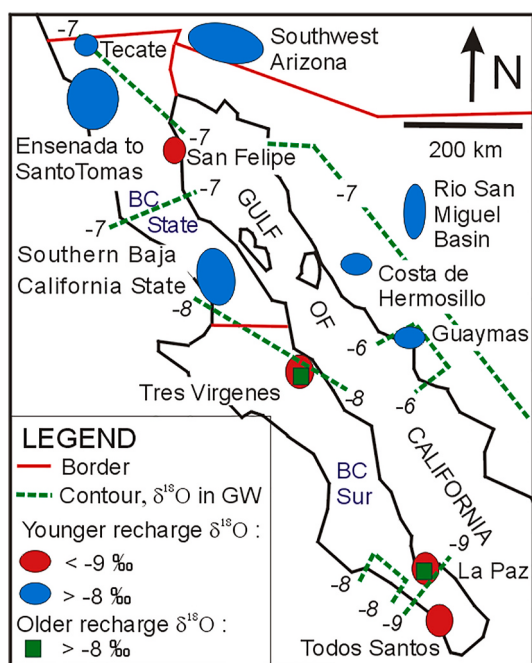


**Fig. 13.** Map of Baja California and adjacent areas, showing distribution of  $\delta^{18}\text{O}$  groundwater (GW) classified by relative age, considering cool groundwater to be younger than geothermal water. Data sources: Ojeda (1998), Szynkiewicz et al. (2008), Kretzschmar and Frommen (2013), Neff (2015), Tamez-Meléndez et al. (2016), Ledesma-Ruiz and Mahlknecht (2017) and Zamora et al. (2021). Green contours of  $\delta^{18}\text{O}$  are based on the groundwater isoscape of Wassenaar et al. (2009).

In southwestern North America, a threshold of 10 percent modern carbon (pMC), uncorrected for post-infiltration effects, serves to distinguish groundwater isotope data corresponding to a positive shift in  $\delta^{18}\text{O}$  and  $\delta^2\text{H}$  recharge during the late-Pleistocene. Speleothem data demonstrate that  $\delta^{18}\text{O}$  in precipitation underwent a positive shift of about 2‰ at 13–15 ka. The distinction in  $\delta^{18}\text{O}$  and  $\delta^2\text{H}$  between late Pleistocene and younger recharge is region-wide, but is not observed in all groundwater basins studied here.

Exceptions to the 10 pMC criterion include Los Angeles basin, where the threshold is 5–8 pMC, and La Paz basin, where a negative isotope shift occurred at a time corresponding to 25–40 pMC in groundwater. No stable isotope shift was observed using the 10 pMC criterion in Ciudad Chihuahua and Pahrangat Valley, Nevada; in these cases, degree of evaporation of recharge increased, but unevaporated source  $\delta^{18}\text{O}$  and  $\delta^2\text{H}$  did not change. Exceptions notwithstanding, a regional pattern of late Pleistocene shift in  $\delta^{18}\text{O}$  and  $\delta^2\text{H}$  in precipitation is indicated.

Confined groundwater with pMC <10 and  $\delta^{18}\text{O}$  and  $\delta^2\text{H}$  values like those of water with pMC >10 may represent recharge prior to a negative isotope shift documented at 51–55 ka in speleothem calcite.

Evidence for isotope shift in recharge may be masked by isotope altitude effects and anthropogenic  $^{14}\text{C}$  from nuclear tests or reactors; other potential complicating factors include delayed melting of late Pleistocene ice and temporal changes in degree of evaporation of river water.

Groundwater recharge mechanisms fall into two patterns related to climate and its effect on evapotranspiration: 1. Winter recharge predominant, with varying degrees of evaporation; 2. Both winter and summer recharge, but only in the wettest months. Pattern 2 occurs at present in the core of the North American monsoon region, where it moved northward, replacing Pattern 1, at the time of the 13–15 ka isotope shift in precipitation.

A later northward progression of climate zones in southern and eastern Baja California led to the replacement of winter-spring recharge (like that still operating in northern Baja California) by summer-fall recharge of precipitation from tropical depressions including hurricanes.

A post-1950 negative shift in  $\delta^{18}\text{O}$  and  $\delta^2\text{H}$  of precipitation is observed in the northern part of the study area, and may be related to advection of moisture from irrigated land in the Central Valley of California.

Further insights should emerge from similar studies in surrounding regions and elsewhere, integrating data collected over multiple groundwater basins. Such advances are likely along the Pacific coast of Mexico, where the evolution and interaction of seasonal weather patterns may resemble those suggested here for Baja California, and in the interior of China, where the area affected by the Indian Summer Monsoon appears to have changed over time (Zhao et al., 2018; Xie et al., 2022). In Baja California, evidence for changes in recharge seasonality is still sparse; detailed studies of additional groundwater basins combining  $^{14}\text{C}$  with  $\delta^{18}\text{O}$  and  $\delta^2\text{H}$  may confirm (or otherwise) the changes suggested here.

## Declaration of competing interest

The authors declare that they have no known competing financial interests or personal relationships that could have appeared to influence the work reported in this paper.

## Data availability

Most data are previously published in cited references. Unpublished data are in Table 2.

## Acknowledgements

Acquisition of many of the author's previously-published data was

funded by the Environmental Isotope Laboratory and the Radiocarbon Laboratory at the University of Arizona. The author gratefully acknowledges insightful reviews from Ian Cartwright and an anonymous reviewer.

## Appendix A. Supplementary data

Supplementary data to this article can be found online at <https://doi.org/10.1016/j.apgeochem.2023.105604>.

## References

- Asmerom, Y., Polyak, V.J., Burns, S.J., 2010. Variable winter moisture in the southwestern United States linked to rapid glacial climate shifts. *Nat. Geosci.* 3, 114–117. <https://doi.org/10.1038/NGE0754>.
- Baillie, M.N., Hogan, J.F., Ekwurzel, B., Wahi, A.K., Eastoe, C.J., 2007. Quantifying water sources to a semiarid riparian ecosystem, San Pedro River, Arizona. *J. Geophys. Res. C Oceans Atmos.* 112, G03S02 <https://doi.org/10.1029/2006JG000263>.
- Beisner, K.R., Paretti, N.V., Tucci, R.S., 2016. Analysis of stable isotope ratios,  $\delta^{18}\text{O}$  and  $\delta^2\text{H}$  in precipitation of the Verde River watershed, Arizona, 2003 through 2014. U.S. Geol. Surv. Open-File Rep, 2016-1053. [https://pubs.er.usgs.gov/publication/ofr2016\\_1053](https://pubs.er.usgs.gov/publication/ofr2016_1053).
- Bills, D.J., Truini, M., Flynn, M.E., Pierce, H.A., Catchings, R.D., Rymer, M.J., 2000. Hydrogeology of the regional aquifer near Flagstaff, Arizona. U.S. Geol. Surv. Wat. Res. Inv. Rep. 142, 00-4122. <https://pubs.usgs.gov/wri/2000/4122/report.pdf>.
- Birkle, P., Portugal Marin, M., Pinti, D.L., Castro, C.L., 2016. Origin and evolution of geothermal fluids from Las Tres Virgenes and Cerro Prieto fields, Mexico: Co-genetic volcanic activity and paleoclimatic constraints. *Appl. Geochem.* 65, 36–53. <https://doi.org/10.1016/j.apgeochem.2015.10.009>.
- Burchuladze, A.A., Chudý, M., Eristavi, I.V., Pagava, S.V., Povinec, P., Sivo, A., Togonidze, G.I., 1989. Anthropogenic  $^{14}\text{C}$  variations in atmospheric  $\text{CO}_2$  and wines. *Radiocarbon* 31, 771–776. <https://doi.org/10.1017/S003382200012388>.
- Carreón-Díazconti, C., Ramírez-Hernández, J., Eastoe, C.J., Martín-Lloeches Garrido, M., Reyes-López, J.A., Rodríguez-Burguén, J.E., Lázaro-Mancilla, O., 2017. Anomalia isotópica en las aguas subterráneas de San Felipe, B.C. Abstract. XXVI Congreso Nacional de Geoquímica, San Luis Potosí, Mexico.
- Cartwright, I., 1982. The potential of groundwater as a geochemical archive of past environments. *Chem. Geol.* 53, 119505.
- Cartwright, I., Currell, M.J., Cendón, D.I., Meredith, K.T., 2020. A review of the use of radiocarbon to estimate groundwater residence times in semi-arid and arid areas. *J. Hydrol.* 580, 124247.
- Clark, I., Fritz, P., 1997. *Environmental Isotopes in Hydrogeology*. Lewis Publishers, Boca Raton, Florida.
- Climate-data.org, 2021. Mexico climate/Mexico weather by month. <https://en.climate-data.org/north-america/mexico>. (Accessed 3 September 2021).
- Coplen, T.B., Kendall, C., 2000. Stable hydrogen isotope and oxygen isotope ratios for selected sites of the U.S. Geological Survey's NASQAN and Benchmark surface-water networks. U.S. Geol. Surv. Open-File Rep. 409, 00-160. <https://pubs.usgs.gov/of/2000/of00-160/>.
- Craig, H., 1961. Isotopic variation in meteoric waters. *Science* 133 (3465), 1702–1703. <https://doi.org/10.1126/science.133.3465.1702>.
- Cunningham, E.E.B., Long, A., Eastoe, C.J., Bassett, R.L., 1998. Migration of recharge waters downgradient from the Santa Catalina mountains into the Tucson Basin aquifer. *Hydrogeol. J.* 6, 94–103. <https://doi.org/10.1007/s100400050136>.
- Dadakis, J.S., 2004. Isotopic and geochemical characterization of recharge and salinity in a shallow floodplain aquifer near El Paso, Texas. The University of Arizona, Tucson, Arizona. Unpublished MS Thesis.
- Darling, B.K., 1997. Delineation of the Groundwater Flow Systems of the Eagle Flat and Red Light Basins of Trans-Pecos Texas. Unpublished Ph.D. dissertation. The University of Texas, Austin, Texas.
- Davidson, M.L., Airey, P.L., 1982. The effect of dispersion on the establishment of a paleoclimatic record from groundwater. *J. Hydrol.* 58, 131–147.
- Davis, G.H., Coplen, T.B., 1989. Late Cenozoic paleohydrogeology of the western San Joaquin Valley, California, as related to structural movements in the central coastal ranges. *Geol. Soc. America Special Paper* 234, 40. <https://doi.org/10.1130/SPE234-1>.
- Davisson, M.L., Criss, R.E., 1993. Stable isotope imaging of a dynamic groundwater system in the southwestern Sacramento Valley, California, USA. *J. Hydrol.* 144, 213–246. [https://doi.org/10.1016/0022-1694\(93\)90173-7](https://doi.org/10.1016/0022-1694(93)90173-7).
- Davisson, M.L., Smith, D.K., Kenneally, J., Rose, T.P., 1999. Isotope hydrology of southern Nevada groundwater: stable isotopes and radiocarbon. *Water Resour. Res.* 35, 279–294. <https://doi.org/10.1029/1998WR900040>.
- Douglas, M.W., Maddox, R.A., Howard, K., Reyes, S., 1993. The Mexican monsoon. *J. Clim.* 6, 1665–1677. [https://doi.org/10.1175/1520-0442\(1993\)006<1665:TMM>2.0.CO;2](https://doi.org/10.1175/1520-0442(1993)006<1665:TMM>2.0.CO;2).
- Druhan, J.L., Hogan, J.F., Eastoe, C.J., Hibbs, B., Hutchison, W.R., 2008. Hydrogeologic controls on groundwater recharge and salinization: a geochemical analysis of the northern Hueco Bolson Aquifer, El Paso, Texas. *Hydrogeol. J.* 16, 281–296.
- Dutton, A.R., 1995. Groundwater isotopic evidence for paleorecharge in the U.S. High Plains aquifers. *Quat. Res.* 45, 221–231. <https://doi.org/10.1006/qres.1995.1022>.

- Earman, S., 2004. Groundwater Recharge and Movement through Mountain-Basin Systems of the Southwest: A Case Study in the Chiricahua Mountains-San Bernardino Valley System, Arizona and Sonora. Unpublished Ph.D. dissertation. New Mexico Institute of Mining and Technology, Socorro, New Mexico.
- Eastoe, C.J., 2007. Report on an isotope study of groundwater from the Mogollon Highlands area and adjacent Mogollon Rim, Gila County, Arizona. Mogollon Rim Water Resour. Manag. Stud.. Available at: [https://www.geo.arizona.edu/sites/www.geo.arizona.edu/files/Eastoe\\_2007\\_MRWRMS.pdf](https://www.geo.arizona.edu/sites/www.geo.arizona.edu/files/Eastoe_2007_MRWRMS.pdf). (Accessed 27 August 2021)
- Eastoe, C.J., Gu, A., 2016. Groundwater depletion beneath downtown Tucson, Arizona: a 240-year record. *J. Contemp Water Res. Educ.* 159, 62–77. <https://doi.org/10.1111/j.1936-704X.2016.03230.x>.
- Eastoe, C.J., Rodney, R., 2014. Isotopes as tracers of water origin in and near a regional carbonate aquifer, the southern Sacramento Mountains, New Mexico. *Water* 6, 301–323. <https://doi.org/10.3390/w6020301>.
- Eastoe, C.J., Towne, D., 2018. Regional zonation of groundwater recharge mechanisms in alluvial basins of Arizona: interpretation of isotope mapping. *J. Geochem. Explor.* 194, 134–145. <https://doi.org/10.1016/j.gexplo.2018.07.013>.
- Eastoe, C.J., Wright, W.E., 2019. Hydrology of mountain blocks in Arizona and New Mexico as revealed by isotopes in groundwater and precipitation. *Geosci. N.* 461. <https://doi.org/10.3390/geosciences9110461>, 10.3390/geosciences9110461.
- Eastoe, C.J., Gu, A., Long, A., 2004. The origins, ages and flow paths of groundwater in Tucson Basin: results of a study of multiple isotope systems. In: Hogan, J.F., Phillips, F.M., Scanlon, B.R. (Eds.), *Groundwater Recharge in a Desert Environment: the Southwestern United States*. Water Science and Application Series, vol. 9. American Geophysical Union, Washington, D.C., pp. 217–234. <https://doi.org/10.1029/029WSA12>
- Eastoe, C.J., Hibbs, B.J., Granados Olivas, A., Hogan, J., Hawley, J., Hutchison, W.R., 2008. Isotopes in the Hueco Bolson Aquifer, Texas, USA and Chihuahua, Mexico: local and general implications for recharge sources in alluvial basins. *Hydrogeol. J.* 16, 737–747. <https://doi.org/10.1007/s10040-007-0247-0>.
- Eastoe, C.J., Hess, G., Mahieux, S., 2014. Identifying recharge from tropical cyclonic storms, Baja California Sur, Mexico. *Ground Water*. <https://doi.org/10.1111/gwat.12183>.
- Eastoe, C.J., Granados Olivas, A., Hibbs, B., 2016. Isotopes and anion chemistry as indicators of groundwater mixing in the Hueco Bolson aquifer, Ciudad Juarez, Chihuahua, Mexico. *Environ. Eng. Geosci.* 22, 195–207. <https://doi.org/10.2113/gsgeosci.22.3.195>.
- Faunt, C.C., Hanson, R.T., Belitz, K., Schmid, W., Predmore, S.P., Rewis, D.L., McPherson, K., 2009. Chapter C. Numerical model of the hydrologic landscape and groundwater flow in California's Central Valley. In: Faunt, C.C. (Ed.), *Groundwater Availability of the Central Valley Aquifer*, vol. 1766. U.S. Geol. Surv. Prof. Pap., California, pp. 121–212. <https://pubs.usgs.gov/pp/1766>.
- Fenneman, N.M., 1931. *Physiography of Western United States*, first ed. McGraw-Hill, New York, USA, p. 534.
- Galloway, D., Riley, F.S., 2006. San Joaquin Valley, California. Largest human alteration of the Earth's surface. U. S. Geol. Surv. Circular 1182 available at: <https://pubs.usgs.gov/circ/circ1182/pdf/06SanJoaquinValley.pdf>.
- González-Hita, L., Mejía-González, M.A., Carteno-Martinez, B., Aparicio-González, J.C., Mañón-Flores, D., 2021. Isotopic composition of rainfall in Baja California Sur, México. *International Jour. Hydrol.* 5 (3), 93–100. <https://doi.org/10.15406/ijh.2021.05.00271>.
- Guay, B.E., Eastoe, C.J., Bassett, R.L., Long, A., 2006. Sources of surface and ground water adjoining the Lower Colorado River inferred by  $\delta^{18}\text{O}$ ,  $\delta\text{D}$  and  $\delta^3\text{H}$ . *Hydrogeol. J.* 14, 146–188.
- Harris, R.C., 1999. Feasibility of using isotopes as tracers of sources of dissolved solids in the upper Gila River, Arizona. *Arizona Geol. Surv. Open-File Rep.* 99–3. [http://repository.agzs.az.gov/sites/default/files/dlio/files/nid1038/offr-99-03\\_uppgilariver\\_report.pdf](http://repository.agzs.az.gov/sites/default/files/dlio/files/nid1038/offr-99-03_uppgilariver_report.pdf).
- Hastings, J.R., Turner, R.M., 1965. Seasonal precipitation regimes in Baja California, Mexico. *Geografiska Annaler, Series A* 47, 204–223. <https://doi.org/10.2307/520662>.
- Hibbs, B.J., Boghici, R.N., Hayes, M.E., Ashworth, J.B., Hanson, A.N., Samani, Z.A., Kennedy, J.F., Creel, R.J., 1997. Transboundary aquifers of the El Paso/Ciudad Juárez/Las Cruces region. Contract Report, Texas Water Development Board, Austin New Mexico Water Resour. Res. Inst., Las Cruces 148.
- Hopkins, C., McIntosh, J., Dickinson, J., Eastoe, C., Meixner, T., 2014. Evaluation of the importance of clay confining units on groundwater flow in alluvial basins using solute and isotope tracers. *Hydrogeol. J.* <https://doi.org/10.1007/s10040-013-1090-0>.
- International Atomic Energy Agency, 2022. Global network of isotopes in precipitation. WISER Database. [http://www-naeweb.iaea.org/napc/ih/IHS\\_resources\\_gnip.html](http://www-naeweb.iaea.org/napc/ih/IHS_resources_gnip.html). (Accessed 5 January 2022).
- Jasechko, S., 2019. Global isotope hydrogeology—review. *Rev. Geophys.* 57, 835–965. <https://doi.org/10.1029/2018RG000627>.
- Jasechko, S., Lechner, A., Pausata, F.S.R., Fawcett, P.J., Gleeson, T., Cendón, D.I., Galewsky, J., LeGrande, A.N., Risi, C., Sharp, Z.D., Welker, J.M., Werner, M., Yoshimura, K., 2015. Late-glacial to late-Holocene shifts in global precipitation  $\delta^{18}\text{O}$ . *Clim. Past* 11, 1375–1393.
- Jasechko, S., Perrone, D., Befus, K.M., Cardenas, M.B., Ferguson, G., Gleeson, T., Luijendijk, E., McDonnell, J.J., Taylor, R.G., Wada, Y., Kirchner, J.W., 2017. Global aquifers dominated by fossil groundwaters but wells vulnerable to modern contamination. *Nat. Geosci.* 10, 425–429.
- Jiang, W., Wang, G., Sheng, Y., Shi, Z., Zheng, H., 2019. Isotopes in groundwater,  $^{2\text{H}}$ ,  $^{18}\text{O}$ ,  $^{14}\text{C}$  revealed the climate and groundwater recharge in the Northern China. *Sci. Total Environ.* 666, 298–307. <https://doi.org/10.1016/j.scitotenv.2019.02.245>.
- Johnsen, S.J., Dahl-Jensen, D., Gundestrup, N., Steffensen, J.P., Clausen, H.B., Miller, H., Masson-Delmotte, V., Sveinbjörnsdóttir, A.E., White, J., 2001. Oxygen isotope and palaeotemperature records from six Greenland ice-core stations: Camp Century, Dye-3, GRIP, GISP2, Renland and North GRIP. *J. Quat. Sci.* 16, 299–307. <https://doi.org/10.1002/jqs.622>.
- Kalin, R.M., 1994. *The Hydrogeochemical Evolution of the Groundwater of the Tucson Basin with Application to 3-dimensional Groundwater Flow Modeling*. Unpublished Ph.D. dissertation. University of Arizona, Tucson, Arizona.
- Kretzschmar, T.G., Frommen, T., 2013. Stable isotope composition of surface and groundwater in Baja California, Mexico. *Procedia Earth Plan. Sci.* 7, 451–454. <https://doi.org/10.1016/j.proeps.2013.03.194>.
- Kulogoski, J.T., Hilton, D.R., Izbicki, J.A., Belitz, K., 2009. Evidence for prolonged El Niño-like conditions in the Pacific during the Late Pleistocene: a 43 ka noble gas record from California groundwaters. *Quat. Sci. Rev.* 28, 2465–2473. <https://doi.org/10.1016/j.quascirev.2009.05.008>.
- Laabs, B.J.C., Munroe, J.S., Best, L.C., Caffee, M.W., 2013. Timing of the last glaciation and subsequent deglaciation in the Ruby Mountains, Great Basin, USA. *Earth Planet Sci. Lett.* 361, 16–25. <https://doi.org/10.1016/j.epsl.2012.11.018>.
- Lambert, S.J., Harvey, D.M., 1987. Stable-isotope geochemistry of groundwaters in the Delaware Basin of southeastern New Mexico. Sandia National Laboratories, Albuquerque, NM. Report SAND 87-0138. Available at : [https://www.wipp.energy.gov/information\\_repository/cra/CRA-2014/References/Others/Lambert\\_Harvey\\_1987\\_Stable\\_Isotope\\_Geochemistry\\_of\\_Groundwaters\\_in\\_the\\_Delaware\\_Basin\\_of\\_SE\\_NM\\_ERMS224150.pdf](https://www.wipp.energy.gov/information_repository/cra/CRA-2014/References/Others/Lambert_Harvey_1987_Stable_Isotope_Geochemistry_of_Groundwaters_in_the_Delaware_Basin_of_SE_NM_ERMS224150.pdf). (Accessed 3 September 2021).
- Leedesma-Ruiz, R., Mahlknecht, J., 2017. Geochemical and isotopic characterization of groundwater in Tecate, Baja California, Mexico. *Procedia Earth Plan. Sci.* 17, 516–519. <https://doi.org/10.1016/j.proeps.2016.12.130>.
- Lo, M.-H., Famiglietti, J.S., 2013. Irrigation in California's Central Valley strengthens the southwestern U.S. water cycle. *Geophys. Res. Lett.* 40, 301–306. <https://doi.org/10.1002/grl.50108>.
- Longmire, P., Dale, M., Counce, A., Manning, A., Larson, T., Granzow, K., Gray, R., Newman, B., 2007. Radiogenic and stable isotope and hydrogeochemical investigation of groundwater, Pajarito Plateau and surrounding areas, New Mexico. Los Alamos Nat. Lab. Rep. LA-14333. Available at: <https://core.ac.uk/reader/71310217>. (Accessed 3 September 2021).
- Lopes, T.J., Hoffman, J.P., 1997. Ages, recharge rates, and hydraulic conductivity of the N aquifer, Black Mesa area, Arizona. U.S. Geol. Surv. Water-Res. Inv. Rep. 96–4190. <https://pubs.er.usgs.gov/publication/wri964190>.
- Mahlknecht, J., Horst, A., Hernández-Limón, G., Aravena, R., 2008. Groundwater geochemistry of the Chihuahua City region in the Rio Conchas basin, northern Mexico and implications for water resource management. *Hydrool. Proc.* 22, 4736–4751. <https://doi.org/10.1002/hyp.7084>.
- Mathany, T.M., Wright, M.T., Beutell, B.S., Belitz, K., 2012. Groundwater-quality data in the Borrego Valley, Central Desert, and low-use basins of the Mojave and Sonoran Deserts study unit, 2008–2010 —results from the California GAMA program. U.S. Geol. Surv. Data Series 659. <https://pubs.er.usgs.gov/publication/ds659>.
- Montgomery, E.L., Associates Inc., 2009. Results of phase 2 hydrogeologic investigations and monitoring program, Rosemont Project, Pima County, Arizona. Vol. 1 Text, tables and figures. Rosemont Copper Company, Tucson, Arizona, USA. Available online at: <https://www.rosemontes.us/documents/012065>. (Accessed 3 September 2021).
- Mayo, A.L., Davey, A., Christiansen, D., 2006. Groundwater flow patterns in the San Luis Valley, Colorado, USA revisited: an evaluation of solute and isotopic data. *Hydrogeol. J.* 15, 383–408. <https://doi.org/10.1007/s10040-006-0079-3>.
- Neff, K.L., 2015. *Seasonality of Groundwater Recharge in the Basin and Range Province, Western North America*. Unpublished M.S. thesis. University of Arizona, Tucson, Arizona.
- Négré, P., Petelet-Giraud, E., 2011. Isotopes in groundwater as indicators of climate changes. *Trends Anal. Chem.* 30 <https://doi.org/10.1016/j.trac.2011.06.001>.
- Newton, B.T., Rawling, G.C., Timmons, S.S., Land, L., Johnson, P.S., Kludt, T.J., Timmons, J.M., 2012. Sacramento Mountains hydrogeology study. New Mexico Bur. Geol. Min. Resour. Open-file Rep. 543. Available at: <https://geoinfo.nmt.edu/publications/openfile/details.cfm?Volume=543>.
- Nickerson, E.L., 2006. Description of piezometers and ground-water-quality characteristics at three sites in the lower Mesilla Valley, Texas and New Mexico. U.S. Geol. Surv. Sci. Inv. Rep. 2005-5248. <https://pubs.usgs.gov/sir/2005/5248/pdf/sir2005-5248.pdf>.
- Ojeda, C.G., 1998. Aquifer recharge estimation at the Mesilla Bolsón and Guaymas aquifer systems, Mexico. Available at: [https://transboundary.tamu.edu/media/1220/1998\\_hueco-Bolsón\\_ojeda.pdf#](https://transboundary.tamu.edu/media/1220/1998_hueco-Bolsón_ojeda.pdf#). (Accessed 3 September 2021).
- Osborn, G., 2004. Great Basin of the western United States. In: Ehlers, J., Gibbard, P.L. (Eds.), *Quaternary Glaciations - Extent and Chronology, Part II*. Elsevier B.V., Oxford, U.K., pp. 63–67.
- Phillips, F.M., Peeters, L.A., Tansey, M.K., Davis, S.N., 1986. Paleoclimatic inferences from an isotopic investigation of groundwater in the central San Juan Basin, New Mexico. *Quat. Res.* 26, 179–183. [https://doi.org/10.1016/0033-5894\(86\)90103-1](https://doi.org/10.1016/0033-5894(86)90103-1).
- Phillips, F.M., Hogan, J., Mills, S., Hendrickx, J.M.H., 2003. Environmental tracers applied to quantifying causes of salinity in arid-region rivers: preliminary results from the Río Bravo, southwestern USA. In: Alsharhan, A.S., Wood, W.W. (Eds.), *Water Resources Perspectives: Evaluation, Management and Policy*. Elsevier Science, Amsterdam, pp. 327–334.
- Plummer, L.N., Bexfield, L.M., Anderholm, S.K., Sanford, W.E., Busenberg, E., 2004. Geochemical characterization of ground-water flow in the Santa Fe Group aquifer system, middle Río Grande basin, New Mexico. U.S. Geol. Surv. Water-Res. Inv. Rep. 03-4131 <https://pubs.usgs.gov/wri/034131>.

- Reichard, E.G., Land, M., Crawford, S.M., Johnson, T., Everett, R.R., Kulshan, T.V., Ponti, D.J., Halford, K.J., Johnson, T.A., Paybins, K.S., Nishikawa, T., 2003. Geohydrology, Geochemistry, and Ground-Water Simulation-Optimization of the Central and West Coast Basins, Los Angeles County, California. U.S. Geol. Surv. Water-Res. Inv. Rep. 03-4065. <https://pubs.er.usgs.gov/publication/wri034065>.
- Rose, T.P., Kenneally, J.M., Smith, D.K., Davisson, M.L., Hudson, G.B., Rego, J.H., 1997. Chemical and Isotopic Data for Groundwater in Southern Nevada. Lawrence Livermore National Laboratory Rep. UCRL-ID-128000, p. 35.
- Schrag-Toso, S., 2020. Isotopes, Geochemistry, Citizen Science and Local Partnerships as Tools to Build upon a Fractured Understanding of the Hydrology of the Northern Patagonia Mountains. Unpublished M.S. thesis. University of Arizona, Tucson, Arizona.
- Smalley, R.S., 1983. An Isotopic and Geochemical Investigation of the Hydrogeologic and Geothermal Systems in the Safford Basin. Unpublished M.S. thesis. University of Arizona. Tucson, Arizona.
- Szynkiewicz, A., Rangel Medina, M., Modelska, M., Monreal, R., Pratt, L., 2008. Sulfur isotopic study of sulfate in the aquifer of Costa de Hermosillo, Sonora, Mexico in relation to upward intrusion of saline groundwater, irrigation pumping and land cultivation. Appl. Geochem. 23, 2539–2558. <https://doi.org/10.1016/j.apgeochem.2008.06.008>.
- Tamez-Meléndez, C., Hernández-Antonio, A., Gaona-Zanella, P.C., Ornelas-Soto, N., Mahlknecht, J., 2016. Isotope signatures and hydrochemistry as tools in assessing groundwater occurrence and dynamics in a coastal arid aquifer. Environ. Earth Sci. 75, 830. <https://doi.org/10.1007/s12665-016-5617-2>.
- Teeple, A.P., 2017. Geophysics- and geochemistry-based assessment of the geochemical characteristics and groundwater-flow system of the U.S. part of the Mesilla Basin/Conejos-Médanos aquifer system in Doña Ana County, New Mexico, and El Paso County, Texas, 2010–12. U.S. Geol. Surv. Sci. Inv. Rep. 2017-5028.
- Thomas, J.M., Welch, A.H., Dettinger, M.D., 1996. Geochemistry and isotope hydrology of representative aquifers in the Great Basin region of Nevada, Utah, and adjacent states. U.S. Geol. Surv. Prof. Pap. 1409-C. <https://pubs.er.usgs.gov/publication/pp1409c>.
- Tucci, R.S., 2018. Using Isotopes and Solute Tracers to Infer Groundwater Recharge and Flow in the Cienega Creek Watershed, SE Arizona Unpublished M.S. Thesis. University of Arizona, Tucson, Arizona.
- Uliana, M.M., Sharp, J.M., 2001. Tracing regional flow paths to major springs in Trans-Pecos Texas using geochemical data and geochemical models. Chem. Geol. 179, 53–72. [https://doi.org/10.1016/S0009-2541\(01\)00315-1](https://doi.org/10.1016/S0009-2541(01)00315-1), 1–4.
- Wagner, J.D.M., Cole, J.E., Beck, J.W., Patchett, P.J., Henderson, G.M., Barnett, H.R., 2010. Moisture variability in the southwestern United States linked to abrupt glacial climate change. Nat. Geosci. 3, 110–113. <https://doi.org/10.1038/NGEO707>.
- Wassenaar, I.I., Van Wilgenburg, S.L., Larson, K., 2009. A groundwater isoscape,  $\delta D$ ,  $\delta^{18}\text{O}$  for Mexico. J. Geochem. Explor. 102, 123–136. <https://doi.org/10.1016/j.gexplo.2009.01.001>.
- Western Regional Climate Center, 2021. SOD USA climate archive. <https://wrcc.dri.edu/summary/>. (Accessed 3 September 2021).
- Winograd, I.J., Friedman, I., 1972. Deuterium as a tracer of regional groundwater flow, southern Great Basin, Nevada and California. Geol. Soc. Am. Bull. 83, 3691–3708. [https://doi.org/10.1130/0016-7606\(197283\[3691:DAATOR\]2.0.CO;2](https://doi.org/10.1130/0016-7606(197283[3691:DAATOR]2.0.CO;2).
- Winograd, I.J., Pearson, F.J., 1976. Major carbon-14 anomaly in a regional carbonate aquifer: possible evidence for megascale channeling, south central Great Basin. Water Resour. Res. 12, 1125–1143. <https://doi.org/10.1029/WR012i006p01125>.
- Winograd, I.J., Thordarson, W., 1975. Hydrogeologic and hydrochemical framework, south-central Great Basin, Nevada-California, with special reference to the Nevada Test Site. U.S. Geol. Surv. Prof. Pap. 712-C 126. <https://pubs.er.usgs.gov/publication/on/ppt712C>.
- Wirt, L., DeWitt, E., 2005. Chapter E. Geochemistry of major aquifers and springs. In: Wirt, L., DeWitt, E., Langenheim, V.E. (Eds.), Framework of Aquifer Units and Ground-Water Flowpaths, Verde River Headwaters, North-Central Arizona. U.S. Geol. Surv. Open-File Rep, 2004-4011. <https://pubs.er.usgs.gov/publication/ofr20041411>.
- Witcher, J.C., King, J.P., Hawley, J.W., Kennedy, J.F., Williams, J., Cleary, M., Bothner, L.R., 2004. Sources of Salinity in the Rio Grande and Mesilla Basin Groundwater. New Mexico Water Resources Research Institute, Las Cruces, New Mexico. Technical Completion Rep. No. 330. <https://nmwrr.nmsu.edu/wp-content/uploads/2015/technical-reports/tr330.pdf>.
- Xie, C., Zhao, L., Eastoe, C.J., Wang, N., Dong, X., 2022. An isotope study of the Shule River Basin, Northwest China: sources and groundwater residence time, sulfate sources and climate change. Jour. Hydrol. Regional Studies 612, 128043. <https://doi.org/10.1016/j.jhydrol.2022.128043>.
- Yang, I.C., Ratnay, G.W., Pei, Y., 1996. Interpretation of chemical and isotopic data from boreholes in the unsaturated zone at Yucca Mountain, Nevada. U.S. Geol. Surv. Water-Res. Inv. Rep. 96-4058. <https://pubs.usgs.gov/wri/1996/4058/report.pdf>.
- Zamora, H., Wilder, B., Eastoe, C.J., McIntosh, J.C., Flessa, K.W., Welker, J., 2019. Evaluation of groundwater sources, flow paths, and residence time of the Gran Desierto pozos, Sonora, Mexico. Geosciences 9, 378. <https://doi.org/10.3390/geosciences9090378>.
- Zamora, H.A., Eastoe, C.J., McIntosh, J.C., Flessa, K.W., 2021. Groundwater origin and dynamics on the eastern flank of the Colorado River delta, Mexico. Hydrology 8, 80. <https://doi.org/10.3390/hydrology8020080>.
- Zhao, L.J., Eastoe, C.J., Liu, X.H., Wang, L.X., Wang, N.L., Xie, C., Song, Y.X., 2018. Origin and residence time of groundwater based on stable and radioactive isotopes in the Heihe River Basin, northwestern China. Jour. Hydrol. Regional Studies 18, 31–49. <https://doi.org/10.1016/j.ejrh.2018.05.002>.
- Zhu, C., 2000. Estimate of recharge from radiocarbon dating of groundwater and numerical flow and transport modeling. Water Resour. Res. 36 (9), 2607–2620. <https://doi.org/10.1029/2000WR900172>.